Power Transmission Engineering®

FEBRUARY
2024

BUILDING A BETTER BEARING

SOLID EDGE 2024

SOLAR ENERGY ADVANTAGES

A CONVERSATION WITH ROGER THOMAS FROM FLENDER

TECHNICAL
Particle-Based CFD Study of Lubrication in Power Transmission Systems

powertransmission.com

Power Transmission Engineering is POWERED by The American Gear Manufacturers Association

Stuck on a Job-site Waiting for a Motor?

We stock hundreds of motors so you can keep your project moving

AutomationDirect carries a full line of AC and DC motors from trusted brands like Toshiba®, U.S. Motors®, WEG®, Leeson®, IronHorse® and Marathon®, at some of the best prices in the industry. In-stock motors are shipped quickly with free shipping on orders over $49*.

Toshiba EQP SD (Severe Duty Motors)

Starting at $376.00

- 230/460 VAC 3-phase from 1/2 - 100 hp
- 1200, 1800, 3600 rpm
- Inverter duty
- Oversized 300-series bearings
- Heavy-duty cast iron construction
- TEFC enclosure with IP55 protection
- Class I, Division 2, Groups A, B, C, D
- NEMA premium efficiency
- UL, UR, CSA
- 3-year warranty

U.S. Motors ACCU-Torq Motors

Starting at $370.00

- 230/460 VAC 3-phase from 1/4 - 10 hp
- 1800 rpm
- Constant torque operation; zero to base speed on vector drives
- 5000:1 speed range
- Constant horsepower operation to 2X base speed
- Optimized for operation with variable speed drives (VFDs)
- Compatible with encoder installation
- NEMA premium efficiency ratings on certain models
- 3-year warranty (1hp and larger)

IronHorse MTS Stainless Steel Washdown-Duty

Starting at $401.00

- Three-phase 208-230/460 VAC from 1/3 to 20 hp
- 1200, 3600 and 1800 RPM
- TEFC or TENV enclosure
- IP69K protection
- Premium Efficiency (EISA Compliant)
- BISSC Certified
- 304 stainless steel frame, end bracket, junction box and hardware
- Class I, Div 2 hazardous locations
- In accordance with NEMA, CSA, UL, and CE
- 2 year warranty

WEG S-Series Rolled Steel Motors and Brake Motors

Starting at $194.00

- Three-phase 208- 230/460 VAC and single-phase 120/240 VAC from 1/4 to 3 hp
- 1200, 3600 and 1800 RPM
- TEFC enclosure with IP55 rating
- Class F insulation
- Premium and Standard Efficiency available
- Certified Class I, Div 2, Groups A,B,C,D
- Brake motors include spring set, solenoid actuated AC brake with manual release lever
- UL, CSA
- 18 month warranty

IronHorse MTRJ Series Jet Pump Motors

Starting at $167.00

- TEFC enclosure
- Class F winding insulation
- Single-phase 120/230 VAC from 1/3 to 2 hp
- Three-phase 208- 230/460 VAC from 1/3 to 3 hp
- 3600rpm
- Built-in thermal protection on single-phase models
- 56J frame with threaded shaft for connection to a jet pump
- 2 year warranty

Also Available

Soft Starters and AC Drives

DC Motors

DC Drives

Research, price, buy at:

www.automationdirect.com/motors

Order Today, Ships Fast!

TOP RATED BY CUSTOMERS

AUTOMATIONDIRECT.com

1-800-633-0405

the #1 value in automation

Power Transmission Engineering®

FEBRUARY 2024

Power Transmission Engineering is POWERED by The American Gear Manufacturers Association

FEATURE ARTICLES

TECHNICAL ARTICLES

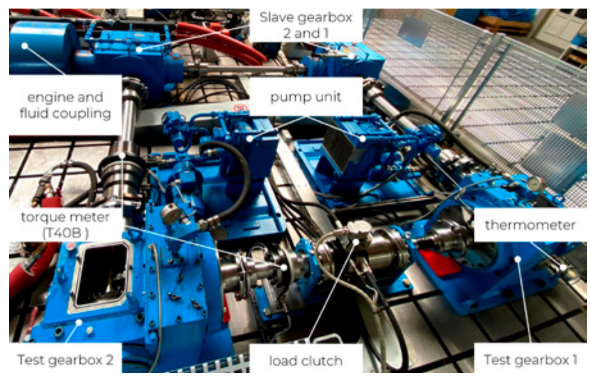

STAY CONNECTED

Follow us on Twitter
twitter.com/PowerTransMag

Connect with us on LinkedIn
linkedin.com/groups/Power-Transmission-Engineering-PTE-2950055

Subscribe Online
powertransmission.com/subscriptions

Vol. 18, No. 1. POWER TRANSMISSION ENGINEERING (ISSN 2331-2483) is published monthly except in January, May, July and November by The American Gear Manufacturers Association, 1001 N. Fairfax Street, Suite 500, Alexandria, VA 22314, (847) 437-6604.

Periodicals Postage Paid at Elk Grove Village IL and at additional mailing offices.

Power Transmission Engineering®
VOL. 18, NO. 1

AI Set to Supercharge Robotic Automation

2023 was an exciting year for innovation. The emergence of artificial intelligence (AI) technologies, such as generative AI, captured global attention and dominated headlines. However, the adoption of generative AI for businesses is still very much in its early stages and questions around how best to harness this technology remain at the forefront of many minds.

powertransmission.com/blogs/1-revolutions/post/9589-ai-set-to-supercharge-robotic-automation

MDSM 2024 Preview (Motor and Drive Technical Track)

Motor & Drive Systems is focused on the latest technical advancements impacting the design, integration, and efficiency of motor, drive systems, and motion control for automation, robotics, manufacturing, and industrial, as well as utilities and automotive applications. Join leading engineers, manufacturers, system integrators, product developers, consultants, and executives and discover how new technologies are improving performance and providing cost savings in a variety of applications.

powertransmission.com/blogs/1-revolutions/post/9595-mdsm-2024-preview-motor-and-drive-technical-track

Rotor Hub and Main Shaft Service and Overhaul

The Faroe Islands' harsh weather and high salt content posed potential challenges to the hub's durability. To ensure its optimal performance, Houghton International utilized reverse engineering capabilities to strip down and comprehensively examine the hub.

powertransmission.com/media/videos/play/251

powertransmission.com

AGMA MEDIA
1840 Jarvis Avenue
Elk Grove Village, IL 60007
Phone: (847) 437-6604
Fax: (847) 437-6618

EDITORIAL
Publisher & Editor-in-Chief
Randy Stott
stott@agma.org

Senior Editor
Matthew Jaster
jaster@agma.org

Senior Editor
Aaron Fagan
fagan@agma.org

GRAPHIC DESIGN
Design Manager
Jess Oglesby
oglesby@agma.org

ADVERTISING
Advertising Sales Manager & Associate Publisher
Dave Friedman
friedman@agma.org

Materials Coordinator
Dorothy Fiandaca
fiandaca@agma.org

CIRCULATION
Circulation Manager
Carol Tratar
tratar@agma.org

MANAGEMENT
President
Matthew Croson
croson@agma.org

FOUNDER
Michael Goldstein founded *Gear Technology* in 1984 and *Power Transmission Engineering* in 2007, and he served as Publisher and Editor-in-Chief from 1984 through 2019. Michael continues working with both magazines in a consulting role and can be reached via e-mail at *michael@geartechnology.com.*

Power Transmission Engineering is somewhat unusual as far as trade magazines go. Rather than focus on a specific industry like, say, aerospace or mining, we focus on all of them—or at least all of them that depend on gears, bearings, electric motors, gear drives and other mechanical power transmission components.

So in any given issue we might have articles that talk about medical devices and mill drives, automobile transmissions and aerospace actuators, or packaging machinery and pumps—a wide range of applications with vastly different requirements. Yet they all depend on mechanical motion. And somebody has to specify the components that make that motion happen. Or somebody has to maintain the equipment to keep a production line running. Either of those tasks requires an in-depth knowledge of the capabilities and options of those components.

That's where we fit in, with our blend of technical articles, technology news, application articles and industry insights.

But sometimes, getting our content in front of those who need it can be a challenge.

So I was hoping that maybe you could help.

Undoubtedly, if you're reading this magazine, you're involved in one or more of these industries. But I'll bet you know some others who could also benefit from this information. Maybe they're part of your everyday team. Maybe they work for your company in a different department. Maybe they work for your customers or suppliers. When I mention things like bearings or couplings or motion control, who comes to mind?

The way you can help is by introducing us. At the bottom of this page is a handy QR-code. Take a picture and text it to a friend. Forward this article to someone you know. If you're reading this online, share it on social media. It's a great way to make sure your friends, colleagues, customers and suppliers are as well informed as you are.

The QR-code leads to our subscription page, which gives you the option to choose what information you want to receive (including this magazine, in either print or digital format, our weekly newsletters, and targeted information like white papers from key suppliers of power transmission components).

And if it's been a while since you've filled out the form yourself, I'd appreciate it if you took a few minutes to update your information and preferences. Keeping our subscriber base up to date is the only way we're able to continue to bring you this information for free.

powertransmission.com/subscribe

Randy Stott
Publisher & Editor-in-Chief

SIEMENS DIGITAL INDUSTRIES

Releases Latest Simulation Software Tools

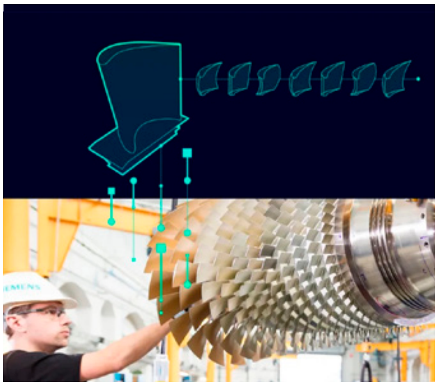

Siemens Digital Industries Software recently released *HEEDS AI Simulation Predictor* software and *Simcenter Reduced Order Modeling* software. These tools empower engineers to tackle the most complex challenges manufacturers face, delivering predictive performance with speed, precision, and efficiency.

Siemens' *HEEDS AI Simulation Predictor* unlocks new possibilities for manufacturers by empowering engineering teams to harness the potential of advanced AI-driven predictive modeling. As a new addition to the *Siemens Xcelerator* portfolio, it can revolutionize design space exploration.

One of the most significant challenges in AI-powered simulation is AI drift, where models extrapolate inaccurately when faced with uncharted design spaces. To address this challenge, *HEEDS AI Simulation Predictor* introduces accuracy-aware AI. This new technology actively self-verifies predictions, aiding engineers to conduct simulations that are not only accurate but also reliable in the context of real-world industrial engineering applications.

"With *HEEDS AI Simulation Predictor*, we have significantly improved various components of the gas turbine, leading to highly optimized designs and accelerated design cycles," said Behnam Nouri, team lead, engineering and platform design, Siemens Energy. "Our thermo-mechanical fatigue predictions have been effectively upgraded to process ~20,000 design members in only 24 hours, yielding a 20 percent improvement in component lifetime. This has allowed us to fully characterize the limits of our existing design space which is required for high-efficiency turbine engines. The *HEEDS AI Simulation Predictor* technology has enabled us to save over 15,000 hours of computational time."

Siemens also introduced *Simcenter Reduced Order Modeling*, new software that harnesses high-fidelity simulation and test data to train and validate AI/ML models. These models then enable engineers to perform predictions in a fraction of a second, transforming the way engineering professionals approach simulation.

"*Simcenter Reduced Order Modeling* lets us accelerate our simulation models to the point where a detailed fuel cell plant model runs faster than real time, with the same accuracy as a full system model," said Jurgen Dedeurwaerder, simulation engineer, Plastic Omnium. "This enables activities such as model-in-the-loop controller development and testing to be done faster, shortening the overall development cycle by around 25 percent. At the same time, it gives us a reliable, IP protected, and cost-effective way to distribute models to other teams, both internally and to our customers to augment their own products and processes, resulting in better quality products delivered to end users."

"*HEEDS AI Simulation Predictor* and *Simcenter Reduced Order Modeling* represent a true breakthrough in simulation technology. They enable our customers to take advantage of benefits of artificial intelligence-driven simulation to speed their exploration of a design space and to do so accurately and robustly," says Jean Claude Ercolanelli, senior vice president, simulation and test solutions at Siemens Digital Industries Software.

sw.siemens.com

RULAND MANUFACTURING

Offers Mountable Shaft Collars with Face Holes

Ruland has released mountable shaft collars with face holes for applications where the shaft collar needs to be directly mounted to a component such as a pulley, sprocket, or metallic plate. The shaft collars are available with drilled face holes that give the user flexibility in mounting hardware, or tapped holes that match the standard screw threading of the collar for ease of installation.

Ruland designs and manufactures face mount shaft collars to have superior fit, finish, and holding power. They have precise face to bore perpendicularity (TIR ≤ 0.002 in. or 0.05 mm), which is critical for mounting applications these shaft collars are typically used in. The groove in the face of the collar identifies the work surface for easy installation. Ruland face mount shaft collars have a burr-free finish, making them an ideal solution for applications in industries such as medical, food, and semiconductor, where contamination is unacceptable. Face mount shaft collars undergo proprietary manufacturing processes to maintain their round bore geometry for tight tolerances, proper installation fit, and improved clamping capabilities.

Ruland offers mountable shaft collars with face holes with drilled or tapped holes. Drilled holes allow for a wider variety of inch or metric mounting hardware to be used. Tapped holes provide a direct interface between the collar, screw, and mated component for the most reliable fit. Either configuration can accommodate socket head, set, or button head screws. The face holes are aligned 180 degrees from each other, allowing the user to install the collar in any orientation.

Ruland manufactures mountable shaft collars with face holes from 1215 lead-free steel for high strength, 2024 aluminum with an anodized finish for lightweight, and 303 stainless steel for corrosion resistance. They are available in one-piece clamp style in bore sizes from 3/8 to 3 inches. and 10 to 80 mm.

ruland.com

PORTESCAP
Expands Flat Motor Portfolio

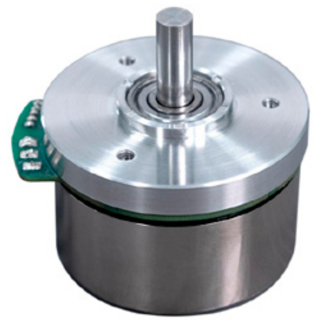

Portescap introduces the 60ECF brushless DC slotted flat motor, the newest frame size to join its flat motor portfolio and a significant expansion of its brushless flat technology capabilities. This 60 mm BLDC motor features a 38.2 mm body length and an outer rotor slotted configuration with an open body design, allowing it to deliver improved heat management in a compact package.

The 60ECF provides up to 298 mNm torque and can be combined with Portescap's R22HT, R26HT, R32, R32HT, and R40 gearheads to deliver extremely high output torque and speed reduction. It is available in both sensored and sensorless options, with the former utilizing hall sensors for easy position control.

This slotted flat motor is a perfect fit for applications requiring high power density and smooth output torque, including those in Aaerospace and defense, robotics, industrial automation, and surgical robotics. Specific examples include electric grippers and exoskeletons, eVtols, and surgical robots.

portescap.com

ORIENTAL MOTOR
Supplies Automation Products for SCARA Robot

Oriental Motor supports the internal designing of application-specific robots with the AZ Series. The AZ Series is a family of motors, actuators, and network drives that feature an absolute sensor, closed-loop control, and easily works with the multi-axis MRC0l controller. This combination of products allows for internally designed and built in-house automation that are designed according to the circumstances and decrease the hurdles in locations where automation wasn't possible; for example, where commercial robots had space restrictions or lack of space inside the equipment, cost limitations, and other barriers.

Automated Sensor Line Assembly Robot

The two actions of transportation between neighboring process equipment and additional positioning have been combined in one horizontal SCARA robot, reducing the processes in order to deal with the issue of restricted equipment width and height as production lines are modularized O.

This robot is arranged beside the production robot. By having the transportation work performed by the production robot and the parts settling work performed by the internal manufacturing robot carried out at the same time, the overall machine time is reduced f). The robot has a simple and compact design comprised of the following, with one unit costing around $8,000 (including the electrical components): an AZ series DC-input motor, a DGII series hollow rotary actuator, a DR series compact linear actuator, an EH series electric gripper, and an MRC01 robot controller. Although there were initially some concerns about how to control and set a multi-axis robot, even inexperienced users were able to make the settings smoothly using *MRC Studio 8*.

`orientalmotor.com`

NSK
Develops High Speed and High Resistance Ball Screws

NSK has developed HTF-SRM ball screws, a high-speed, heat-resistant version of its high-load drive ball screws, ideal for high-cycle, thin-wall molding in electric injection molding machines.

NSK is exhibiting this product at the IPF Japan 2024 International Plastics Fair and plans to begin accepting orders in April 2024, with a global rollout to follow. NSK aims to achieve annual sales of 500 million yen by fiscal 2026 for this product.

The newly developed SRM (Smooth Return Metal coupling) recirculation system and heat-resistant components achieve the industry's highest level of operating speed and heat resistance. The permissible d-n value[1] is 200,000, a 40 percent improvement over NSK's conventional high-speed HTF-SRC ball screws. The maximum operating temperature is 90°C and momentary maximum temperature is 100°C, both of which are 20°C higher than NSK's conventional products.

The external dimensions of the screw and nut are the same as those of the HTF-SRC model, eliminating the need for design changes when upgrading.

`nsk.com`

STAFFORD MANUFACTURING
Introduces Shaft Collars and Mounts

Shaft collars and mounts that can be adjusted without tools, plus handles and thumb screws to convert standard shaft collars to quick-adjust types, have been introduced by Stafford Manufacturing Corp. of Wilmington, MA. Stafford Quick-Adjust Products feature the Flip-Lok with a split hub and an integral adjustable clamp, Staff-Lok Lever-Actuated shaft collar, and the Python Flange Mounting Collar with a 6-hole bolt pattern and keyway. Suitable for a wide range of linear and low RPM rotary applications, these quick-adjust products can be easily repositioned by hand without tools.

Available in inch and metric bore sizes from 1/2" to 2-1/2", depending upon product, Stafford Quick-Adjust Products are made from aluminum anodized black and can be supplied as specials in colors or made from steel and stainless steel with modifications to OEM requirements.

For applications using rope, the SlipKnot is molded from ABS plastic and allows for precise location as a grip, locator, or stop. Stafford Quick-Adjust Products, Grip and Go Handles, and Thumbscrew knobs are priced depending upon configuration and quantity.

staffordmfg.com

SKF

Expands Wireless Solution for Condition Monitoring

SKF has expanded its portfolio of condition monitoring solutions with the SKF Enlight Collect IMx-1-EX sensor solution. Wireless monitoring of assets helps predict machine failure before it can escalate into a serious problem, such as an unscheduled shutdown. This can deliver multiple benefits, including reduced costs and a more sustainable operation of equipment.

The new sensor is part of the well-established SKF Enlight Collect IMx-1 wireless eco-system and certified according to ATEX and IECEx standards for use in Zone 1 and Zone 2 classified hazardous areas. The sensor works in tandem with the SKF Enlight Collect IMx-1-EX gateway, which is certified for use in Zone 2.

"The IMx-1 wireless solution, in combination with our analytical software, provides state-of-the-art information and insight into the health of rotating assets, now also in hazardous areas, and further expands SKF's plantwide condition monitoring eco-system," says Fredrik Larsson, condition monitoring technologies manager at SKF.

The new solution has the same form, fit and function as the safe-area rated SKF Enlight Collect IMx-1. All devices have full compatibility, allowing customers to build a network of monitored assets across hazardous and safe areas.

The sensor uses innovative measurement capabilities to provide advanced insights into asset health, including early detection of bearing damage. Like other IMx-1 sensors, they create a 'mesh network', enabling them to relay data between one another. This allows data to be routed around obstacles such as pipework—which can block signals for conventional line-of-sight systems. This facility means that data can be sent over greater distances than would otherwise be possible.

skf.com

IGUS

Develops Finger Gripper for Cobot

Igus has developed a finger gripper for the ReBeL cobot. The ReBeL can now perform a variety of simple humanoid tasks with the new low-cost robotic hand.

Robots have become an integral part of industry and are increasingly finding their way into small and medium-sized companies in the form of cobots, such as the ReBeL. They sort, pick, and move with the help of cameras, suction devices, and gripper systems. The newly launched finger gripper for the ReBeL cobot can perform humanoid tasks. It is made entirely of self-lubricating plastics and is, therefore, cost-effective, and easy to integrate.

With the ReBeL, Igus has brought a compact and lightweight cobot onto the market, which allows for a cost-effective way to start working with robotics. It is ideal for assembly tasks, quality inspections, and jobs in the service sector. For the robot to perform tasks, it requires grippers and suction devices. For this purpose, Igus offers a wide selection of suitable end effectors from various manufacturers on the *RBTX.com* marketplace.

"As the ReBeL is very light and inexpensive with a weight of around 8 kg and a price starting at $6,899, it is often used in humanoid applications. For this reason, we have received several customer requests for a robot hand that can be easily connected to the ReBeL via plug and play," explains Alexander Mühlens, head of the low cost automation business unit at Igus GmbH.

This is why Igus has now developed a particularly cost-effective ReBeL finger gripper, which is available for as little as $2,760. The humanoid hand is compatible with all ReBeL models. It is controlled via DIO at the tool center point, making it easy to integrate and suitable for various applications. A unique feature of the finger gripper is that it can imitate a person's hand movements.

"The ReBeL can take on a wide range of simple humanoid tasks and applications with the new low-cost hand. We are thinking of such fields as research and development at universities as well as tasks in the catering or entertainment industries," says Mühlens.

All components, including the flange, cables, and control unit, are provided directly from Igus. This gives the customer a solution that is 100 percent compatible. Self-lubricating high-performance plastics keep the price low. The plain bearings in the joints made of iglide polymers are not only cost-effective and self-lubricating, but also ensure smooth and precise movements of the individual fingers. Extensive tests in the company's own 3,800-square-metre laboratory guarantee the longevity of the humanoid hand. They are incredibly flexible and can be controlled via various interfaces, including USB, TTL (5V) serial, and internal scripting.

In addition to the finger gripper, Igus offers other products for the ReBeL environment. These include, for example, fire-resistant smoke hoods, a 7th axis, gripper sets, adapter plate sets, energy supply systems, a finished workstation, and connection cables.

igus.com

Solid Edge 2024 Focuses on Performance and User Experience

A Q&A on the latest software update

Siemens Digital Industries Software

Solid Edge is a portfolio of affordable, easy-to-use software tools that address all aspects of the product development process. *Solid Edge* combines the speed and simplicity of direct modeling with the flexibility and control of parametric design—made possible with synchronous technology. The following Q&A discusses *Solid Edge 2024* with Dan Staples, vice president, mainstream engineering, Siemens Digital Industries Software.

What does digital transformation mean for small and medium sized business?

Digital transformation is the unleashing of the power of intelligent product design, and that's at the core of it. It's the integration of digital technologies into all aspects of your engineering business, but what that looks like can vary based on the size of the company.

Siemens sponsored a study with industry analyst IDC, which focused on small and medium-sized business (SMB) manufacturing and digital transformation. We surveyed key decision makers at hundreds of SMBs around the world asking them about digital transformation, their strategies, plans and recent progress.

Since the study was first conducted in 2017, and then again at the end of 2021, we can see the trends over the past few years. Here are a couple of highlights. In 2021, 72 percent of the advanced SMBs surveyed believed that digital transformation helps level the playing field for small businesses versus their larger competitors—the last time the survey was taken, it was 63 percent.

Plastic Fischer is working to reduce plastic waste in rivers, so it does not pollute our oceans and has adopted the Siemens Xcelerator portfolio to help scale its operations and bring the benefits of digital transformation to its product development and lifecycle management. (Plastic Fischer GmbH)

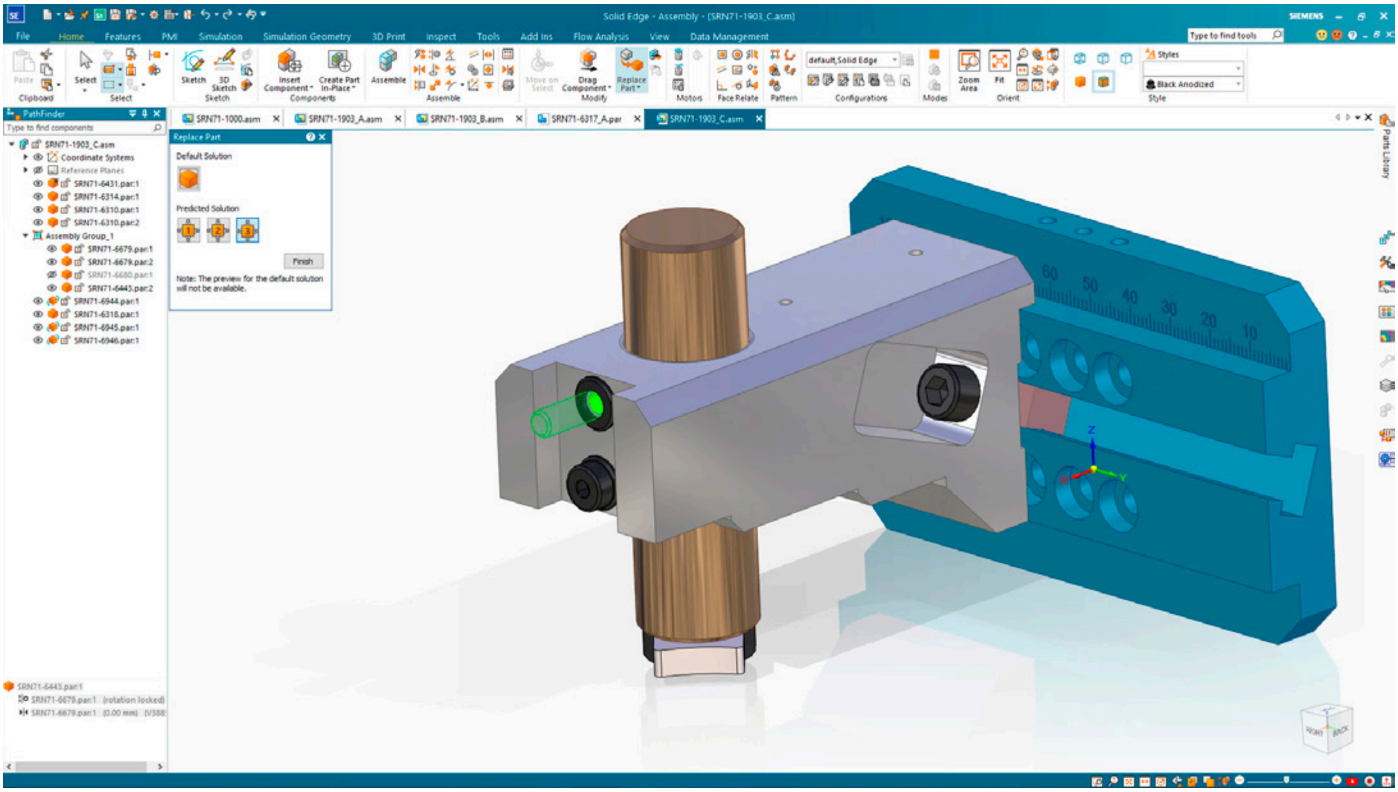

Leverage the power of Artificial Intelligence (AI) to save time when replacing parts in an assembly. With the improved "Replace Part" command, Solid Edge can now intelligently suggest assembly relationships and predict valid alternative solutions.

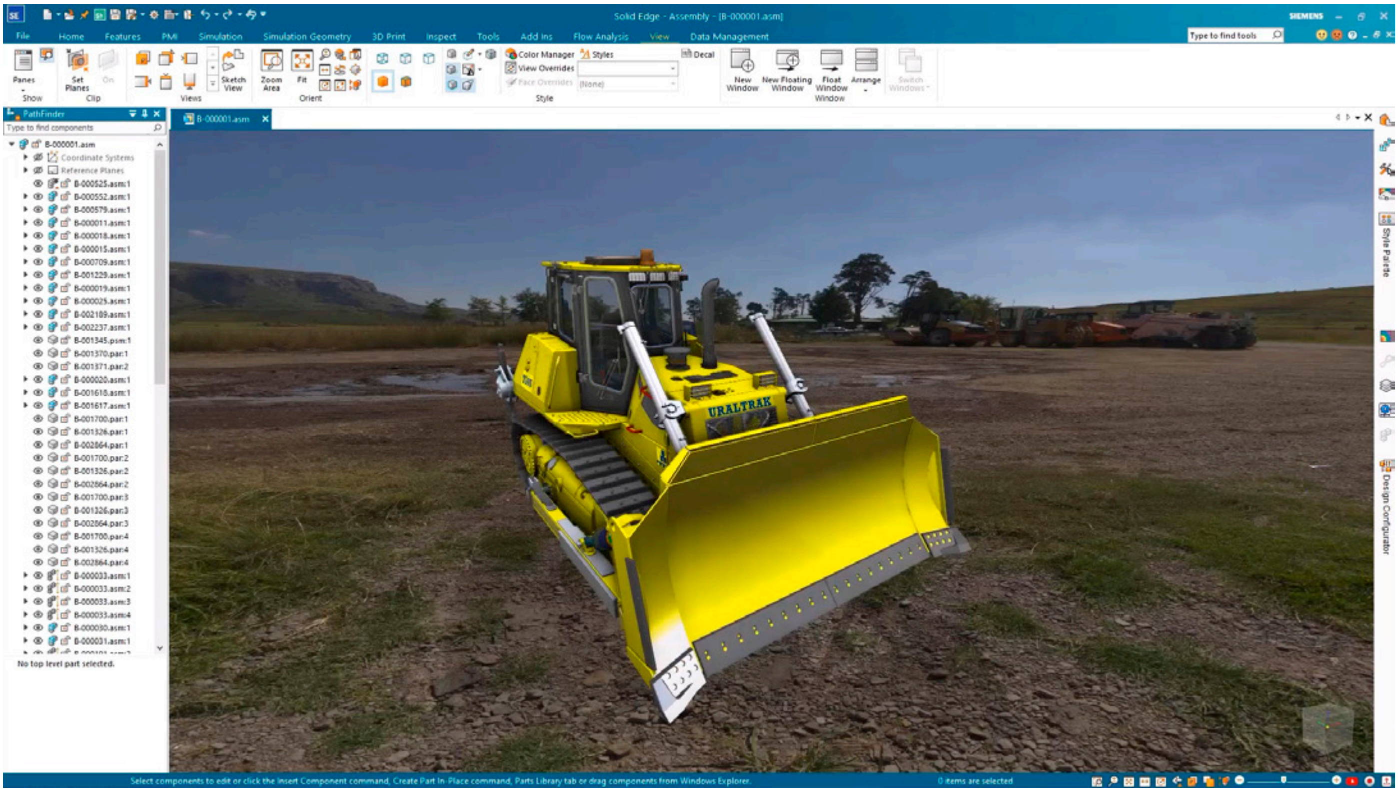

Solid Edge enables manufacturers to create a comprehensive digital twin of their products and includes solutions for mechanical design, electrical design, simulation, manufacturing, and technical publications.

IDC also asked about their investments during the global pandemic and related disruptions, and 80 percent of SMBs maintained or increased their digital transformation budgets—a great measure of how important these investments are.

Second, the survey asked about technology priorities. Among these, cloud computing and software as a service, or SaaS, stood out. Nearly a third of SMB manufacturers surveyed said that they were prioritizing cloud computing SaaS solutions, and nearly half said that these categories would be a technology priority in the next 12 months. IDC notes that the cloud is the great enabler for collaboration and analytics.

Are the same benefits true for startups?

Even smaller companies like startups are leveling the playing field through digital technologies that help them collaborate more effectively. A great example is an amazing startup called Plastic Fischer. They're helping the planet by keeping the oceans clean—by capturing plastic waste in rivers before it reaches the ocean. See story here:

powertransmission.com/articles/9520-siemens-digital-provides-software-solutions-for-plastic-fischer

We're also investing in the next generation of engineers through a new program called "Hour of Engineering." This program demystifies engineering and promotes it as a desirable career path by providing real-world engineering challenges connected to global goals. It helps students build engineering habits of mind, like creativity, systems thinking and collaboration.

How does *Solid Edge* fit into the *Siemens Xcelerator* portfolio?

Siemens Xcelerator is an integrated portfolio of industrial software and services, and it really blurs the boundaries between traditionally standalone domains like electronics, mechanical and software. It ties all those disciplines together into a single seamless whole. And, frankly, *Siemens Xcelerator* really starts with *Solid Edge*—it's a key part of the *Siemens Xcelerator* portfolio and is squarely focused on the requirements of small and midsize manufacturers.

Solid Edge enables manufacturers to create a comprehensive digital twin of their products and includes solutions for mechanical design, electrical design, simulation, manufacturing, and technical publications. It also includes solutions for data management for all the technical data that's created and consumed when supporting the comprehensive digital twin.

Ultimately, *Solid Edge* facilitates collaboration both within manufacturing companies and with external resources, including suppliers and customers—that makes it the on-ramp to digital transformation and enables us

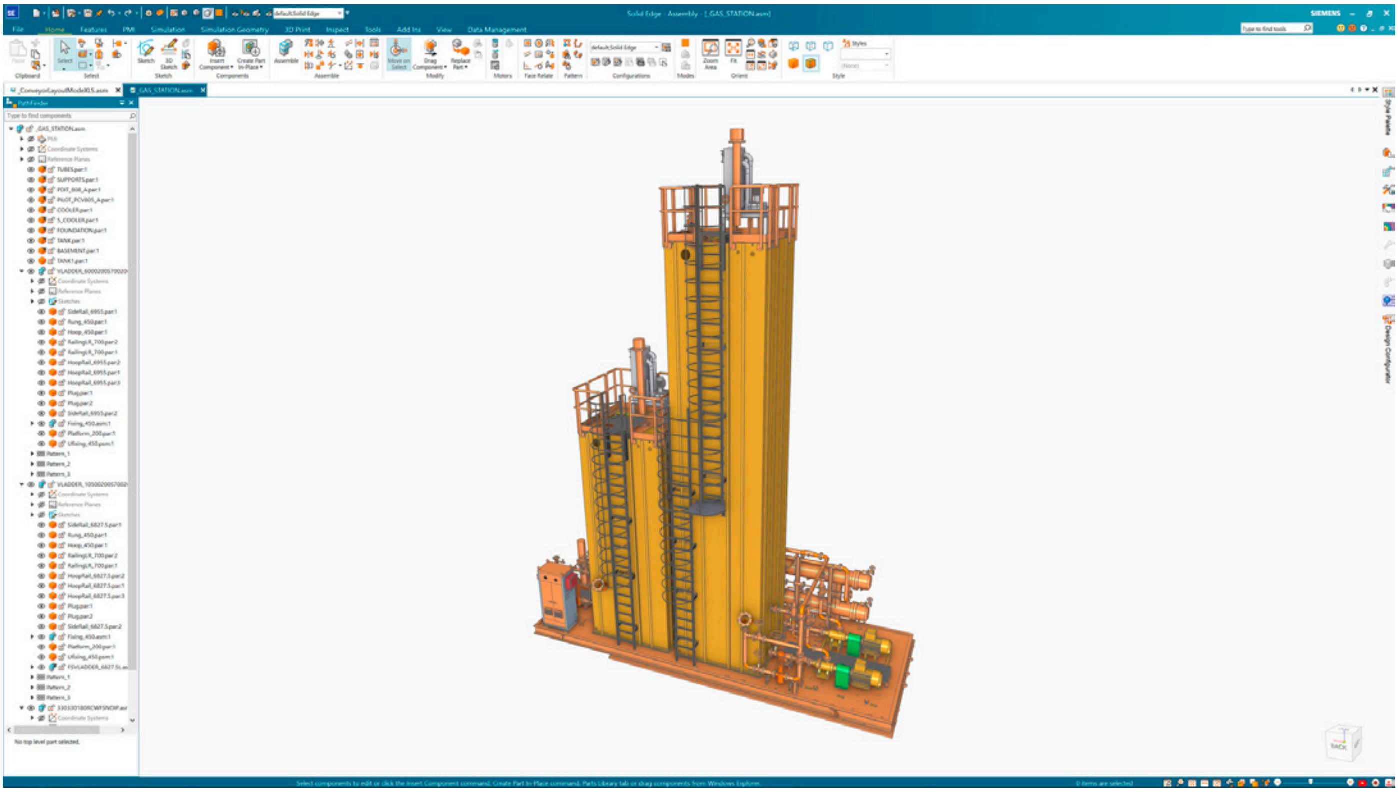

Insert and manipulate preconfigured models quickly and easily at no cost with Solid Edge Design Configurator. As intelligent datasets with predefined rules, a vast array of preconfigured models can be inserted and automatically adjusted to match the assembly to help simplify workflows and improve productivity.

to help customers accelerate their digital transformation with *Solid Edge 2024*.

What are the highlights of the *Solid Edge 2024* update?

With this year's release we continue to push the boundaries of product development technology by empowering users to design more intelligently across every aspect of product development. With a continued focus on the user experience and large assembly performance, *Solid Edge 2024* introduces functionalities and enhancements to automate and speed design as well as collaboration. A few highlights I'm proud of—the nine times faster graphical performance, artificial intelligence (AI) driven assembly relationships, great advancements in intelligent dimensioning, and so much more.

What have the beta testers said about this update?

As with every year, our beta customers have already had the opportunity to experience *Solid Edge 2024*. Summing up the general feedback nicely is the comment from Carsten Oestmann, the leader of the CAD team at industrial machinery specialist, Focke & Co:

"Each year *Solid Edge* gets better and better. This year, everything is faster. With faster reaction times in large assemblies, everything feels more fluid. I can't wait to share it with my team. Large assemblies now load and rotate at least 50-percent faster. That's the type of performance that can improve every one of our workflows."

Artificial intelligence is a hot topic across the technology world—how is Siemens using it in the 3D design and engineering world?

One of the key highlights for this update is our continued work applying AI technologies in the design process to speed things up—removing repetitive work and taking advantage of machine learning to help our users be more productive. A great example is the new AI-enhanced 'Replace Part' command that uses AI to predict solutions for replacing a component occurrence within an assembly. The AI looks at the geometry of the part a user is replacing alongside the new part and presents viable solutions—they then click the correct solution and they're done. It saves effort, can speed up product iterations and redesigns by not having to create those relationships manually, and works equally well with standard, imported parts, as it does with native data.

What do your customers think about using AI as part of their day-to-day activities?

AI, when implemented in tools like *Solid Edge*, can remove repetitive tasks and free up resources in an engineering team. The reality is that CAD users are often carrying out tedious, repetitive tasks—so why not let the computer do that? The best answer is to

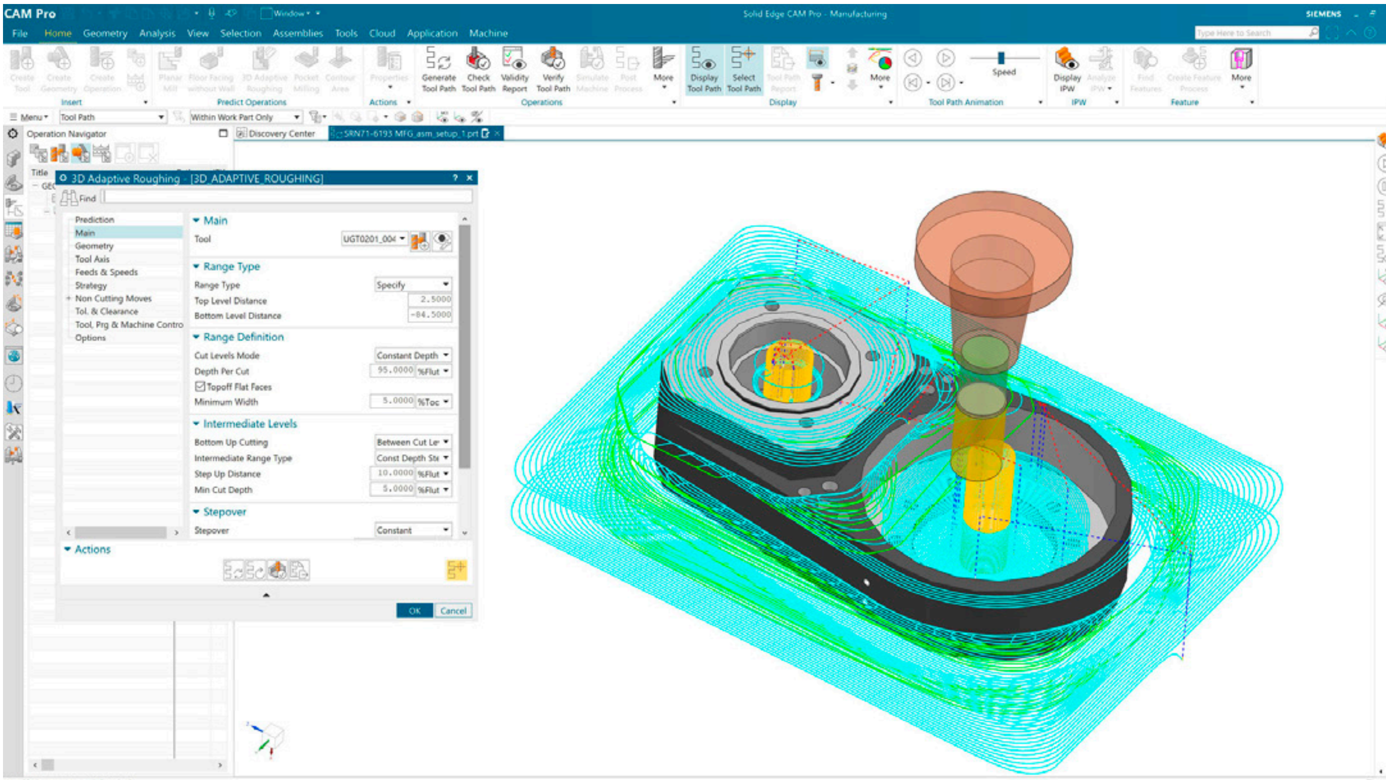

Faster programming and more efficient machining cycles are now possible due to the introduction of 3D Adaptive Roughing operations. High-speed, bottom-up cutting strategy enables methodical removal of material between cut levels by re-cutting the stock at decreased levels by stepping upward.

quote another beta tester, David Iverson of separable reciprocating gas compressor manufacturer, Ariel Corporation, who loves that it allows his team to focus on the real challenges.

"*Solid Edge 2024* helps us work smarter and be more productive. Incorporating AI into our design processes will cut down time spent on tedious tasks, letting us do more of the fun stuff," Iverson said.

AI is also useful in an industrial context when used alongside other advanced technologies—look at the work we have been doing for the past few years on generative design, where we use simulation technology to automate concept design, based on loads and constraints in a product. AI can change how we design, but it needs to sit alongside our existing technologies—and with capabilities such as synchronous technology, we believe that Siemens has the optimal portfolio of software that can help users overcome real-world barriers to innovation by taking advantage of AI assisted design.

Alongside the headline-grabbing AI updates—how else are you improving users' productivity?

Whether it's improving our large assembly performance by nine times for this release or rethinking how we can accelerate frame and tube design, enabling users to go faster and with more intelligence built into their product models is fundamental.

A notable example of how *Solid Edge 2024* supports improved productivity is the new 'Trim Tubes' command. Frame design is something that happens in many of our customer sites, whether that's industrial machinery, factory cell design or motorsport. This new tool allows users to identify overlaps very quickly in a framework and trim those tubes, readying them for manufacture and fabrication with a few simple clicks. It might not be flashy or headline grabbing, but for those involved with frame design daily this update is a game changer.

Speeding up the design process is great, but how is Siemens helping the wider manufacturing enterprise?

The challenges facing today's manufacturers are many, ranging from supply-chain complexity to the drive for innovation, to customers looking for greater choice and customizability. The last challenge is something that our customers are telling us is a key pressure point—where the increase in product variants is presenting a challenge not only from an engineering point of view, but across the enterprise in terms of sales support. To help our customers overcome this challenge, we have worked on *Solid Edge Design Configurator*, our rules-

> "Solid Edge enables manufacturers to create a comprehensive digital twin of their products and includes solutions for mechanical design, electrical design, simulation, manufacturing, and technical publications."
>
> *Dan Staples, Siemens Digital Industries Software*

based design capability. Firstly, we are now able to include preconfigured models in *Solid Edge Design Configurator*, so the engineering team can quickly and easily place intelligent datasets of common items such as ladders, conveyors and enclosures that adapt according to design rules—again, something that is repetitive, and ideal for automation.

Extending the use of rules-based design further, we've also introduced *Solid Edge Design Configurator Connect*. This is a user-friendly web-based configurator that manages the most complex pricing and product configurations, allowing users to configure online in any browser simply and easily. It then automatically generates sales documentation, including 3D models, which allows customers to offload some of the work that would traditionally be done in the engineering office and move it to the hands of the sales and marketing team.

youtu.be/Lj5Hi5-m0ls?si=hEl6_PHdHM3f_nNo

How does Teamcenter Share tie all this together?

Teamcenter Share builds on our previous cloud-based data sharing and collaboration capabilities, previously known as *Xcelerator Share*, a common service offered as part of any subscription to *Siemens Xcelerator* portfolio and allows the sharing of data and collaboration around that data wherever it is needed. *Teamcenter Share* is now embedded in *Solid Edge 2024* and provides subscribers to *Solid Edge SaaS* with a streamlined collaboration platform to help them work with their entire team, including partners and customers.

Through *Teamcenter Share* users can view, interact with, and collaborate around, a wide variety of data formats (from both Siemens and third-party systems). It also offers built-in data management capabilities: files can be checked in or out and access always controlled, projects managed, and tasks assigned—all from within the *Solid Edge* interface without the need to use another application. If a partner or team member needs access but does not have *Solid Edge* available, the same *Teamcenter Share* experience is also available via a web browser, on any device, opening collaboration for those that need it when they need it.

One of our customers, Hall Designs, uses *Solid Edge* to design vehicles for the off-road racing industry. They use *Teamcenter Share* to better communicate with their clients during the iterative design process. Their clients can easily view, measure, and mark up CAD models within the 3D development space using a browser-based interface accessible from any device. In addition, collaborators can view and comment on files, view model sections and cutaways, take measurements, change units, and add text-based annotations—all in real time for other team members to see. This eliminates the need for back-and-forth emails with PDF attachments for those who can't open CAD files. Hall Designs reports that *Teamcenter Share* enabled them to reduce the time it took to share designs by 75 to 80 percent and accelerate the product revision process by 20 to 25 percent.

solidedge.siemens.com/en/solutions/products/complete-product-development-portfolio/solid-edge-2024/

PTE

For Related Articles Search

software

at *powertransmission.com*

Vesconite Bearings Invests in Energy Efficiency in South Africa

Factory reduces reliance on power grid to enhance 24/7 operation

Matthew Jaster, Senior Editor

South Africa has an abundance of sunshine with more than 2,500 hours of sunshine a year and solar-radiation levels between 4.5 and 6.5 kWh/m² per day.

On-site at Vesconite Bearings, where the company is installing a comprehensive solar energy solution.

Vesconite Bearings, a global supplier of bearing and wear materials located in Johannesburg, South Africa, is taking strides towards sustainability and environmental responsibility by implementing a comprehensive solar energy solution. The initiative, spearheaded by Factory Manager Robin Crabb and CEO Dr Jean-Patrick Leger, involves a significant investment in solar infrastructure to reduce the factory's reliance on the power grid and make substantial progress in becoming more environmentally friendly.

South Africa's power utility has been struggling to supply consistent power to residential and industrial consumers for about a decade, according to Crabb. This situation has worsened of late, with most consumers in December 2023 facing two to six hours a day without electricity.

"Some industrial consumers have responded to the energy crisis by investing in energy solutions that can ensure that they can supply customers with manufactured goods that require energy to produce. Industrial consumers have invested in short-term solutions to provide power, including expensive-to-operate diesel generators, but are increasingly realizing that they need to spend a significant amount of Capex to invest in longer-term solutions to a power crisis that shows no likelihood of ending any time soon," Crabb said.

For Vesconite Bearings, which already had a 65 kW test solar solution as well as a diesel-generating solution, the continued sustainability of the company required the investment in an expanded solar power solution to supply a greater proportion of its daylight energy requirements.

South Africa has an abundance of sunshine with more than 2,500 hours of sunshine a year and solar-radiation levels between 4.5 and 6.5 kWh/m2 per day. In the Free State, the province in which Vesconite Bearings factory is located, compressed natural gas must be trucked in, making it similar in price to diesel.

Crabb said solar energy, by far, is the most logical alternative energy choice for the area.

"The region is flat and dry, so hydro is not a possibility. There are no prevailing winds for most of the year, making wind energy a non-starter. Thus, none of these options are practical or cost effective. As such, the sun is the preferred and most reliable source of energy that can be implemented by individual companies with ease," he added.

As of mid-November 2023, Phase I of the project was 80 percent complete, with the installation of steelwork on concrete slabs to support 325 kVA of solar panels. Simultaneously, Phase II is underway, encompassing the installation of an additional sub-station, the installation and commissioning of two generators, inverters with a capacity of 700 kVA, and a 500 kVA uninterrupted power supply (UPS) system.

According to Crabb, "Making the sub-station live is a significant step forward, with approximately 25 percent of Phase II already completed."

The completion of Phases I and II was targeted for the end of 2023, contingent on timely equipment deliveries from suppliers. Phase III aims to double the solar capacity by an additional 325 kVA. Challenges in steel supply may influence the timeline, but Vesconite Bearings remains committed to its sustainability goals.

Additionally, consideration is being given to purchasing a 1 MW

Solar Power Outlook Here in the States

The U.S. Energy Information Admninistration (EIA) forecasts that the United States will generate 14 percent more electricity from solar energy than from hydroelectric facilities in 2024, according to its Short-Term Energy Outlook (STEO). This forecast is driven by continued growth in new utility-scale and small-scale solar facilities. For the first time in September 2022, the United States had more solar-generated electricity than hydroelectric generation on a monthly basis, according to Electric Power Monthly. That month, U.S. solar power plants and rooftop solar generated about 19 billion kilowatthours, (kWh) compared with 17 billion kWh from U.S. hydropower plants. Solar power outpaced hydropower again in summer 2023 due to exponential growth in installed solar capacity. From 2009 to 2022, installed solar capacity increased at an average rate of 44 percent per year, and installed hydroelectric capacity increased by less than 1 percent each year. EIA expects annual solar generation to surpass annual hydropower generation in 2024 for the first time. In 2019, annual wind generation surpassed annual hydropower generation. The growth of U.S. solar and U.S. wind generation are following a similar pattern, both largely following growth in installed capacity. (*eia.gov*)

For Related Articles Search
solar energy
at powertransmission.com

Vesconite is aware that its ability to become a supplier of choice in the future will depend on whether its environmental priorities are aligned with those of its customers.

battery system, enabling the storage of solar energy for peak consumption times during the night. This investment aligns with Vesconite Bearings' vision for its 'lights-out' facility, intended to operate 24/7 for large-volume order production, circumventing challenges posed by load-shedding from South African electricity provider Eskom.

To enhance security, the company is also installing a 1.8 m electric fence around the solar system.

Leger expressed optimism about the project's potential impact, stating, "We aim to reduce dependence on traditional energy sources, cut costs, and significantly decrease our carbon footprint."

Vesconite Bearings is confident that these solar investments will fortify the company's resilience against energy challenges and contribute to a greener, more sustainable future for South Africa and beyond.

When the system is complete, a third to a half of Vesconite's daily energy requirements should be catered for, supplemented by diesel generators in times of inclement weather. At this time battery storage solutions remain so capital-intensive that nighttime energy requirements (approximately two-thirds of daytime requirements) will remain a major challenge.

South African companies face energy challenges that require energy independence. Other global companies are facing energy challenges in the form of rising costs, due to the war in Ukraine, and the lack of energy availability in some cases. More important, though, are the commitments that many companies have made to have zero carbon emissions by 2030 to mitigate and prevent the devastating effects of climate change.

"Vesconite Bearings is similarly concerned with the impact of climate change and believes that each individual and corporation needs to do as much as possible to reduce the harm that their production and consumption have on the environment," Crabb said.

Vesconite Bearings is aware that its customers are increasingly requiring supplier information on a raft of issues, including environmental sustainability. While some customers continue to make purchases based on price alone, Vesconite is aware that its ability to become a supplier of choice in the future will depend on whether its environmental priorities are aligned with those of its customers.

For Vesconite Bearings, the moral imperative of doing less harm to the planet, and becoming aligned with its customers' environmental commitments, is reinforced by the fact that investing in its solar solutions will reduce its overall expenditure on energy. This will also mean that it does not have to pass on a portion of rising energy costs to its customers.

"Customers who were affected by supply vulnerabilities during COVID are also increasingly looking at their supply chains and trying to ensure that their suppliers can continue to produce goods even in the worst conditions. The company remains dedicated to achieving its environmental and operational objectives through innovation and responsible business practices," Crabb added.

vesconite.com

PTE

Building a Better Bearing

An innovative look at analysis, condition monitoring, mounting and maintenance.

Matthew Jaster, Senior Editor

With an "all-hands on deck" approach to maintenance today, engineers require the latest tools and technologies in the form of new software/apps to make MRO tasks easier. Turns out, technology is allowing your smartphones, tablets and computers to track bearing reliability and performance with an emphasis on sustainability, longevity and analysis.

SKF Bearing Assist App Offers Improvements

Every year, there are millions of bearing failures caused by incorrect mounting. Overcoming this can deliver multiple benefits to owners (operators) of rotating machinery, including reduced costs related to maintenance, fewer breakdowns, as well as a more sustainable operation of the machinery.

The *SKF Bearing Assist* app, on a smartphone or tablet, supplies step-by-step guidance, replacement instructions and an improved way to document and trace each replacement bearing. A detailed checklist ensures that each necessary step, such as planning and preparing the job and measuring associated components, has been completed.

Geri Palinkas, product manager, *Bearing Assist*, SKF caught up with *PTE* to discuss updates to the company's bearing app. Palinkas said there have been three major updates in the latest version:

1. The definition of bearing position has been added which helps the technician to keep products separated. This also provides more structure and clarity in the documentation.
2. The checklist has been refined to reflect the workflow in a more correct way and is placed as the centerpiece of the replacement activity. In the previous version the checklist was a sub task for a bearing.
3. SKF has also added a PDF preview so that the user can look at the result without sending it with email.

Regarding mounting performance, the app provides guidance for the user which creates confidence and speed. "The checklist also helps to prevent the user from forgetting important steps in the workflow. The documentation helps when investigating any future problems and can act as a reference in future replacements or in training," Palinkas said.

The *SKF Bearing Assist App* is centered around the workflow for the entire replacement process and not only the physical dismount and mount. In a replacement job the workflow is represented with a very clear checklist that guides the user and prevents important steps from being forgotten.

"There is also a digital measurement protocol that automatically makes the user aware of tolerance breaches. It's no longer mandatory (but still possible) to reference the job to a machine and finally it's easy to document the replacement with images and notes. The documentation can then be opened and shared as a nicely formatted PDF report," Palinkas said.

How is *Bearing Assist* changing MRO in general? Through the app SKF offers any industrial company a digitalized process and method to improve the planning, execution, and documentation of bearing replacements.

In the future, Palinkas said the app will offer more guidance in the different steps of the workflow as well as smoother and faster documentation of the job. SKF will also drive towards more self-service and self-education by helping with identifying bearings suited for remanufacturing, finding correct tools and suitable training, and suggesting help for alignment and condition monitoring.

The following is a list of additional apps that are noteworthy for rotating equipment:

- *Bearing Select*, is a tool for bearing selections and calculations is redesigned for a better user experience (*skfbearingselect.com/#/bearing-selection-start*)
- *Axios* is a simple, wireless and scalable end-to-end predictive maintenance solution from SKF and AmazonWebServices (*skf.com/group/products/condition-monitoring-systems/surveillance-systems/wireless/axios*)
- *IMx-1* can now also be used in hazardous areas (*skf.com/group/news-and-events/news/2023/2023-11-21-new-wireless-sensor-solution-from-skf-enables-automated-machine-monitoring-in-hazardous-areas*)
- The newly released *SKF Microlog Analyzer dBX* is the most advanced large-screen vibration analyzer offered by SKF today (*skf.com/group/products/condition-monitoring-systems/portable-systems/microlog-analyzer-dbx*)

"We are also working on new functionality in *Bearing Assist* bundled as an enterprise offer helping mid-size and large enterprises with structure, traceability and insights when it comes to bearing replacements," Palinkas said.

skf.com/us/support/engineering-tools/bearing-assist

Romax Software Updates Bearing Capabilities

Hexagon recently released *Romax DT 2023.1*, as part of the full Romax software suite. Bearing specialists require independent tools supplying innovative rolling element bearing analysis. These tools will provide the insight needed to design and select bearings for optimum performance and durability, as part of a whole system model. Whether selecting the appropriate bearings for a concept design, designing a custom bearing for a specific application, or performing root cause analysis of a bearing failure, engineers need reliable prediction of bearing performance to make key decisions. In addition, bearing suppliers and OEMs must be able to collaborate and share data with each other, while being independent and preserving valuable IP.

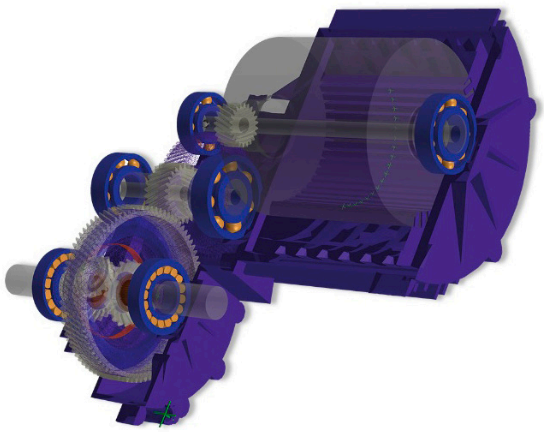

Romax Spin, for example, features detailed modeling of rolling bearings, fast and intuitive modeling of full drive systems, and advanced contact algorithms that accurately capture the non-linear behavior of bearings. Users can calculate load and stress distributions, film thickness, standard ratings such as ISO 281 and ISO/TS 16281 and run dynamic simulations to study phenomena such as skidding and cage dynamics.

Dr. Michael Platten, Senior Product Manager—Romax, explains some of the highlights from the 2023.1 release of the Romax software suite which includes updates to *Romax Spin*.

Modeling and Usability: The 2D Worksheet now shows which bearings have 1D raceway connections. This allows users to quickly check all the bearings in a model to see which are configured to have 1D raceway flexibility and which do not. (Note, a similar visual check if bearings have 3D (FE) raceway flexibility is enabled.)

Journal Bearings: The operating temperature of the journal bearing lubricant film can now be directly specified. In previous versions, the journal bearing operating temperature was determined as the mean temperature of its shaft and housing. This can now be overridden with a custom value, for example, obtained outside of Romax software, and this temperature will affect the lubricant viscosity used in the journal bearing component calculations.

Rolling Element Bearings: Multi-lobe ovalization and custom bearing ring distortion. Rolling bearings may be radially deformed by design from a circular shape to a bi-lobe, tri-lobe, or other geometry to limit skidding. Previously it was possible to define ovalization (i.e. bi-lobe shape) in Romax software. Now, this has been extended to allow multiple lobes and custom shapes, primarily to enable the modeling of tri-lobe raceways, but more lobes or an entirely custom shape are also enabled. This allows parametric investigation of the applied raceway distortion and its impact on load and stress distribution and ring deformation.

Previous bearing dynamics capability in *Romax Spin* has a simplified representation of cages. The cages are considered rigid and they were only allowed to rotate about their own axis. This development addresses one of these limitations by adding lateral and tilt degrees of freedom to the cages, in addition to the rotation about their own axis. This would allow engineers to analyze the lateral motion of a cage and its stability by looking at the whirl orbits under various operating conditions.

A new bearing catalog from NTN has been added to Romax software. It is available alongside existing bearing catalogs and offers matching functionality. The catalog data is based on the General Rolling Bearing Catalog issued separately by NTN. As with other bearing supplier catalogs, limited data has been provided by NTN and the rest of the bearing internal and advanced data has been estimated by Romax.

The EP Additives setting is now reported alongside the lubricant name and level of contamination in the reports ISO 281 and ISO/TS 16281 Results to give the user more context when reviewing bearing life results. This feature minimizes the effort required to check the status of EP additives on individual bearings.

The EP Additives setting is now reported alongside the lubricant name and level of contamination in the reports ISO 281 and ISO/TS 16281 Results and Bearing Certification Report (ISO 281 and ISO/TS 16281) to give the user more context when reviewing bearing life results. This feature minimizes the effort required to check the status of EP additives on individual bearings.

Learn more here: *simcompanion.hexagon.com/customers/s/article/Whats-New-Romax-DT-2022-1*

Schaeffler's OPTIME Ecosystem Balances Plant Assets

OPTIME is an easily scalable condition monitoring system that consists of wireless, battery-powered vibration sensors, a cellular gateway and an app to visualize the resulting data. This information, which is captured by the sensors, is analyzed using proprietary algorithms that draw on Schaeffler's technical expertise, its extensive library of physical models developed and refined over many decades, and the experience in condition monitoring that Schaeffler has built up during its bearing servicing operations.

OPTIME is designed to provide advance warning of potential damage to machines such as electric motors, fans and pumps. It also offers early notification of imbalance, misalignment, and loose-fitting components. The OPTIME mobile app displays trends in graph format and visualizes the severity of incidents using traffic light colors, alarm states and other information. Assets can be grouped according to the user's requirements, and their condition can be presented in a range of user group-specific views. With OPTIME, in-house maintenance personnel and external service contractors receive specific recommendations regarding the steps required to remedy any issues, enabling them to easily plan their maintenance activities, manpower requirements and spare parts procurement in a timely and cost-effective manner.

Frank Mignano, Schaeffler condition monitoring sales manager for North America, recently discussed some of the new updates and future considerations for OPTIME:

How the OPTIME Ecosystem works

The Ecosystem consists of many elements including user interfaces, cloud and analytics, existing customer ecosystems, other Schaeffler measuring devices, condition monitoring, mesh network, smart lubrication and more.

The latest updates include vibration/temperature sensors for all "balance of plant" assets; a Smart Lubricator which reports status of single-point lubricators—full, empty, days left, clogged, excessive temperature; a cellular gateway for unimpeded connectivity to the Schaeffler Cloud; a Cloud application for implementing Schaeffler-proprietary diagnostic algorithms on the mountains of collected data—thereby converting data into actionable information; a web dashboard and smart phone application to help manage the asset health and maintenance planning activities.

In addition, the ProLink multi-channel monitoring solution, designed for more critical assets, can also be sent to the same Cloud so the end user can manage all their asset health information in one place.

Food and Beverage Boiler Fan Application

A machine critical to the food and beverage industry—boiler fan in the fryer area—can cease production on any failures. Prior to enabling the "learning mode" alarm set points, OPTIME uses the ISO velocity recommendation (based on machine size) which alerted the customer to a higher-than-normal vibration on the machine. Utilizing the "Expert Viewer" application, the customer was able to identify the peaks in the demodulation vibration plot as lining up with the outer race frequency of the bearing. The peaks were prevalent in both the standard acceleration and the demodulation signal processing technique, indicating an advanced defect. Maintenance plans were scheduled for the fan resulting in cost savings of at least 20,000 CDN. The pilot OPTIME project identified this issue within two weeks of initial install.

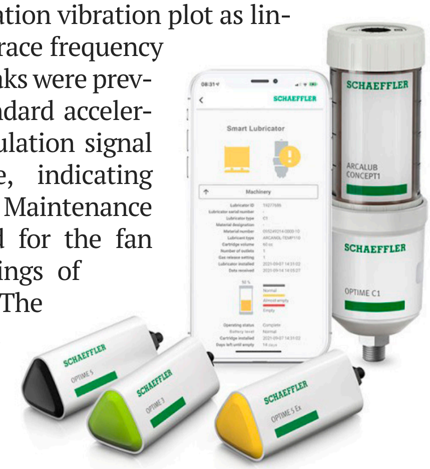

Future Considerations

Mignano offered a few planned features for future updates including: a simple drop-in, 4-port smart lubricator—connecting directly to the Ecosystem; lubrication on condition from the 4-port lubricator; dynamic mode and high dynamic mode for intermittently operating machinery (cranes, etc.) as well as significant, automated diagnostic enhancements (AI, machine learning) and electric motor-specific monitoring capabilities.

medias.schaeffler.us/en/monitor/optime-ecosystem

PTE

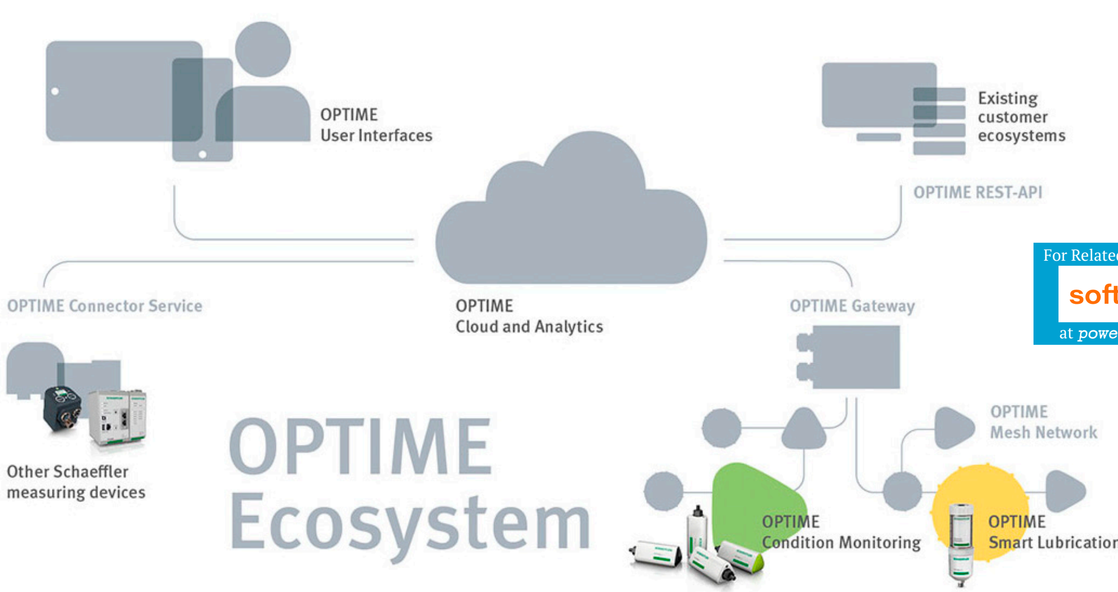

When off the shelf just won't do.

With our enormous variety of standard components and custom machining capabilities, a custom-designed and manufactured gearbox for specific applications is something we do all the time.

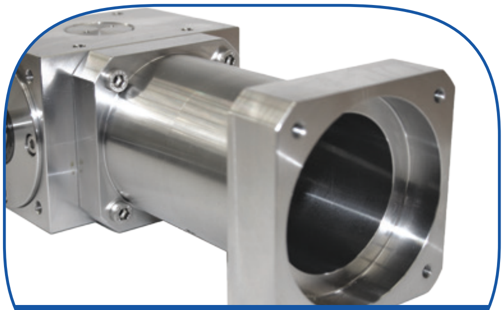

Custom Flanges

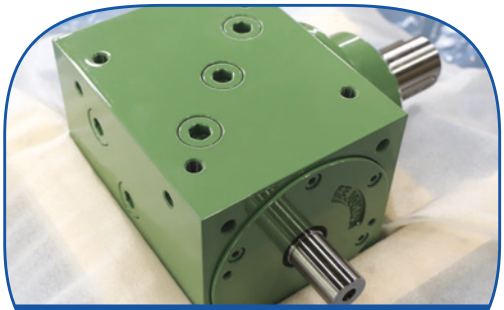

Custom Paint

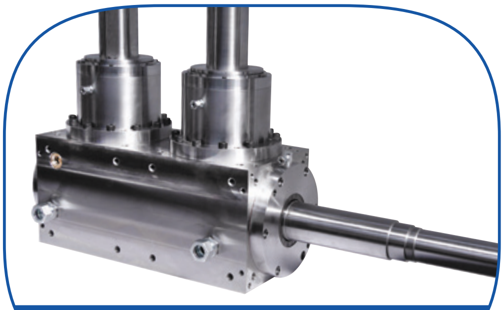

Complete Redesigns

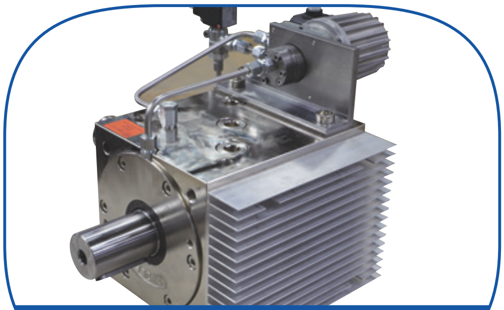

Gearbox Cooling

DIEQUA Corporation

180 Covington Drive
Bloomingdale, IL 60108 USA

630-980-1133

www.diequa.com

Motion Control and Power Transmission Drive Components

Advancing Motion and Power: A Conversation with Roger Thomas from Flender Corporation

From the "Ask the Expert" stage at Motion + Power Technology Expo 2023

Aaron Fagan, Senior Editor

In an exclusive interview conducted at the Motion + Power Technology Expo 2023 in Detroit, marketing director Roger Thomas of Flender Corporation sheds light on the Flender One helical gear unit. Our discussion delves into product development, its link between product design and digital services, and the overarching commitment of Flender toward sustainability. The Flender One's unique features, such as AIQ integration for intelligent monitoring and Metaperform gearing philosophy, are explored in detail, offering insights into its applications, gear ratio ranges, and design considerations. Roger also addresses questions about the larger housing surface, its relationship to integral cooling, and the retrofitting capabilities of the AIQ system to previous generations of Flender gearboxes. As Flender looks to the future, Roger outlines the company's vision of continued innovation, emphasizing a commitment to energy efficiency, waste reduction, and achieving CO^2 neutrality by 2030. Join us in unraveling the complexities of motion and power transmission technology with a leader at the forefront of change, Flender Corporation.

***Roger Thomas, Marketing Director, Flender Corporation,* roger.thomas@flender.com**

Please walk us through the development of the Flender One and the link between product design and digital services.

It is encouraging to see that more and more of our customers and stakeholders want to reduce energy and carbon footprint for a sustainable future. With the same goal, Flender saw an opportunity to develop a revolutionary gear unit that meets customer needs and incorporates the latest technologies.

The new Flender One helical gear unit offers the perfect balance between thermal capacity and efficiency, ease of use and technological sophistication, and torque and transmission range, allowing it to meet customer requirements precisely. Due to its extremely low power dissipation, the gear unit pays for itself through reduced energy costs alone—in most cases, within three years.

Incorporating AIQ, our new gear unit intelligence with integrated sensor technology minimizes downtime as it monitors performance, records, and displays performance data for local analysis, decision-making, and process control.

How would you profile the typical applications for Flender One gearbox?

Typical applications include paper productions, pumps, compressors, mixers, agitators, and water turbines, to name a few.

How many gear ratio ranges are available?

103 transmission ratios from 1 to 7.1 are available for each of the 11 gearbox sizes. This provides the densest range of transmission stages available on the market and allows us to match the desired rotation speed for maximum efficiency and with a speed fit of nearly 99 percent.

Could you please define Metaperform gearing for the uninitiated?

Metaperform is a design philosophy we use at Flender to develop new products. It focuses on primary design objectives and helps us maintain focus throughout the development. The primary design objective of Flender One was to save power and energy. The aim is achieved by designing a more uniform path of contact and improved roll-off characteristics of the gears, an innovative housing design for improved heat dissipation, a wide range of transmission ratios for speed fit, and digitalization for performance monitoring.

The gearboxes have a 35 percent larger housing surface than previous models. Is that related to integral cooling?

You are correct. The surface area and the thermal capacity of Flender One have increased significantly compared to the predecessor products. The rid design is integral to efficient cooling, resulting in better heat dissipation and unparalleled thermal capacity. This eliminates the need for over-dimensioning to increase the gear unit's cooling capacity while reducing the need for additional cooling measures.

One might assume that would increase the weight or footprint of the units, but that isn't so, correct?

Although the housing surface is larger, the footprint is the same, but the weight is less.

Please tell us about AIQ.

AIQ is Flender's intelligent sensor incorporated in each Flender One when it ships from the factory. It provides insight into the operational performance of the gear unit as it monitors vibrations, temperature, and speed measurements with the overall objective of avoiding unplanned downtime and saving energy. It also calculates the remaining oil life by providing full-time monitoring, alert generation, and recommended actions if a parameter exceeds alarm thresholds.

Can AIQ be retrofitted to the previous generation of Flender gearboxes?

AIQ can be retrofitted to previous generations of Flender gearboxes. We only need customer information about the application and the type of connectivity desired to determine the correct sensor.

What is on the horizon for Flender?

We are proud of the reputation for superior quality that we have earned throughout our 120-year history. Flender One is an example of leveraging our acquired product knowledge and industry expertise to develop innovative products to deliver optimal value and customer experience.

We will continue to develop products that save energy, labor, and waste to achieve CO^2 neutrality by 2030.

We want to be recognized as the partner of choice for a sustainable future.

flender.com

PTE

Flender One is a 2022 iF Award-winning platform. Available as single-stage and multistage solutions, these gear units are suitable for over 100 applications.


High Performance Bevel Gearboxes
The Tandler Spiral Bevel gearbox is both precise and ideal for demanding applications where robustness and high torque density are required.
• 9 sizes
• 15 ratios
• Low backlash
• Customizable
DIEQUA Corporation
diequa.com/pte
800-363-2145


Custom Engineering
Prototype Work
Precision Machining
Assemblies and Standard Components
GEARS | PULLEYS | SHAFTS |
BEARINGS | COUPLINGS |
FASTENERS | CUSTOM GEAR BOXES
Nordex® INCORPORATED
ISO9001:2015 & AS9100D,
ITAR Registered,
NIST.SP800-171R1,
Trace Certified,
Class 100 clean room
Nordex.com
Sales@nordex.com | Eng@nordex.com
800-243-0986 | 203-775-4877


Inline Helical Speed Reducers
An extremely compact design provides highly reliable, space saving performance for the most demanding applications.
• 14 sizes, 1 - 75 HP
• Multi-stage Ratios
• NEMA, IEC, or Servo Motor Adapters
• High Efficiency & Low Backlash
• Multiple Mounting Configurations
DIEQUA Corporation
diequa.com/pte
800-292-9135


Come check out AGMA's FIRST
Electric Vehicle (EV) course!
REGISTER TODAY!
agma.org
AGMA
EV AUTOMOTIVE TRANSMISSION DEVELOPMENT
2.0 CEUs
April 23-25, 2024
Ann Arbor, MI
Registration Deadline
April 15
This course will cover all aspects of gearbox concept, development, design, and through the initial stages of analysis as related to product requirements.

Engineering sMart

Your resource for the latest in great ideas from our advertisers. Check this section every issue for sMart Engineering ideas and technology.

For information about advertising contact

Dave Friedman
(847) 437-6604 | *friedman@agma.org*

Subscribe TODAY

IT's FAST. IT's EASY.
IT keeps YOU in the KNOW.
powertransmission.com/subscribe

Torque Limiters Promote Human Safety in Automatic Door Systems

Exploring friction and ball torque limiter designs in motorized turnstiles, sliding doors and other public-facing systems.

Alex Bronzini, President, Comintec North America

Without the right mechanical safety measures in place, automated door systems—such as turnstiles, revolving doors and sliding doors—can put human users at risk. These systems are commonly found in commercial and public buildings like airports, shopping centers, hospitals, transit hubs and sports arenas to manage the flow of people, enhance security and provide easy access for individuals with disabilities. As part of the mechanical countermeasures, these systems include torque limiters, which ensure the door always operates within safe limits, preventing accidents.

In addition to safeguarding people, the torque limiters used in automatic door systems protect the equipment itself. Too much torque can damage the motor, gears, and other components in the motorized system, requiring frequent, costly repairs or part replacement. Torque limiters can therefore extend the life of these components by minimizing damage and wear and tear. Their ability to disengage and slip prevents obstructions or obstacles in the door, be it people or items, from continuously straining the motor. Allowing the motor to stop and reset can save both time and money by protecting the equipment and minimizing wear and tear-related downtime.

At ComInTec, we developed torque limiters for use in these mission-critical safety applications. Here's a deep dive into units we made specifically for motorized door systems, including the ways they safeguard both people and equipment during operation.

Automatic systems, which must operate around hundreds to thousands of people each day, can be a recipe for disaster without the proper safety measures in place.

For Related Articles Search
torque limiters
at powertransmission.com

What is a Torque Limiter?

A common power transmission component, torque limiters protect machinery and equipment from excessive torque or overload conditions by limiting the amount of torque transmitted through a drivetrain or power transmission system. If the torque exceeds a predetermined threshold, the torque limiter will disengage or "slip," interrupting the power transmission temporarily. This function allows the system to reset, resolving the overload condition.

In addition to motorized door systems, torque limiters are found in many industries and equipment, including conveyors, forming machines, winches, agricultural equipment and automotive systems.

Due to their simple yet effective design, torque limiters offer a wide range of benefits:

Reliable operation: Because they rely on mechanical components to detect and limit torque, torque limiters are reliable and easy to maintain. There are no electronic components or complex software systems that can fail.

Cost-effective: Compared to complex electronics, torque limiters are more cost-effective and are typically less expensive to repair or replace.

Immediate response times: As soon as there is a change in torque, torque limiters will disengage the drivetrain almost instantaneously, providing fast protection against overloading, jamming or other hazards.

High load capacity: Torque limiters can handle very high loads and are preferred in a range of industrial applications, including heavy machinery and equipment. Our largest standard units can handle

The EDF/F series is a ball torque limiter, which consists of two halves: a driving member and a driven member that are separated by a set of steel balls housed in grooves on both members.

The DF series is a friction torque limiter, which relies on friction between two surfaces to limit the amount of torque that is transmitted through the system.

Torque limiters fill an important role by limiting the amount of torque that can be transmitted through the door system.

up to 120,000 Nm, while standard DF torque limiters can handle up to 23,000 Nm. In typical turnstile applications, the torque required to release the system is quite low to facilitate egress in case of emergency.

The Role of Torque Limiters in Automatic Door Systems

Automatic door systems are one important application for torque limiters. These systems must be able to operate around high volumes of people, providing safety, reliability, robustness and, in many cases, an aesthetically pleasing design. Important for both the protection of the system and the protection of its users, various kinds of doors benefit from torque limiters in different ways.

The torque limiter may slip and disengage because of different causes, one of them being obstructions or detected obstacles. These applications may include motorized turnstiles for people waiting in long lines, public access hatches, walkways, revolving doors, and swing doors, residential gates for private access, sliding or folding doors in automotive and locomotive applications.

Other automated door systems require controlled opening and closing to properly manage foot traffic. These applications that can benefit from torque limiters include tripod turnstiles for checking tickets at events or managing passenger flow in subways, large turnstiles for controlling passenger flow in places that require a high degree of security—such as airports and other transit hubs.

These dynamic systems, which must operate around hundreds to thousands of people each day, can be a recipe for disaster without the proper safety measures in place. Torque limiters fill this important role by limiting the amount of torque that can be transmitted through the door system. If the torque exceeds the set limit, the limiter will slip, preventing further torque transmission. Torque limiter slippage can prevent automatic doors from becoming immobile and denying access to users or potentially trapping them.

ComInTec Torque Limiters

ComInTec developed two units—the DF friction torque limiter and EDF/F ball torque limiter—which feature a compact and easy-to-install design, high durability, and minimal maintenance even after a high number of cycles. These components can also be integrated into existing door systems without altering the design, keeping uptime high.

The DF series is a friction torque limiter, which relies on friction between two surfaces to limit the amount of torque that is transmitted through the system. The basic design consists of two rings, which are mounted on either side of the drive shaft. If the transmitted torque exceeds the threshold, the material between the plates will begin to slip, which stops the load from rotating and prevents damage to the drive unit. In motorized door applications, the DF series provides end-of-stroke slippage, quietly intervening without disconnecting the movement.

Additional features include a simple, economic mechanical design, silent overload without vibration, protection in both rotation directions, asbestos-free friction discs, precise torque-setting via adjusting the locking ring, and up to 23 kilonewton-meters (KNm) of torque and 140 mm bore diameters.

The EDF/F series is a ball torque limiter, which consists of two halves: a driving member and a driven member that are separated by a set of steel balls housed in grooves on both members. When the input shaft rotates and exceeds the torque limit, the balls are forced out of their grooves, causing the driving member to slip past the driven member, stopping the transmission. In motorized door applications, the EDF/F series will switch off the control motor to the system in the event of an accidental impact. It will also allow the unlocking of the movement in emergency situations.

Additional features of this unit include reduced torsional backlash by the ball drive, maintenance-free for long-lasting operation, use in damp and oily environments, and up to 1,450 Nm of torque and 55 mm bore diameters.

Learn More About Torque Limiters

Torque limiters like the DF and EDF/F series provide reliable, cost-effective protection against torque-related hazards in a wide variety of machinery. At the same time, their mechanical simplicity, immediate response time and high load capacity make them a popular choice for maintaining safety in motorized door applications.

`comintecusa.com`

PTE

Particle-Based CFD Study of Lubrication in Power Transmission Systems Using Local Refinement Techniques

Benjamin Legrady, Dive Solutions GmbH

In the field of mechanical engineering, addressing challenges related to energy efficiency, raw material consumption, and environmental impact has become increasingly critical. Industries are constantly pushed to develop innovative products and optimize existing ones to comply with strict regulations governing power consumption and emissions. The rise of electrified engines, hybrid solutions, and alternative fuel concepts, such as hydrogen or e-fuels, further underscores the need for advancements in drivetrain components. These components play a vital role in transmitting the power generated by an engine to the road surface. While current designs achieve conversion rates of up to 97–99.5 percent of mechanical input power to usable output power, there is still significant potential for further improving the efficiency of gearboxes (Ref. 1). Enhancing gearbox efficiency not only reduces heat dissipation for a given power output but also enables the design of more compact cooling components. Optimizing lubrication flow in gearboxes can also minimize the amount of oil required to reduce friction between gears and dissipate heat from drivetrain components. With the advent of water-based lubricants, the innovation process also takes place on the material side. However, it is crucial to address emerging losses that become more pronounced at higher rotational speeds and lower loads, which are typical conditions for automotive transmissions operating at their top gear ratio (Ref. 2).

By gaining a comprehensive understanding of and effectively controlling the lubrication flow within transmissions, significant advancements can be made toward achieving more efficient and environmentally friendly gearboxes. This paper aims to investigate the mechanisms and origins of hydraulic losses in bevel-geared gearboxes, with the ultimate goal of identifying opportunities for constructive measures to optimize losses and increase overall efficiency. Through the utilization of the Smoothed Particle Hydrodynamics (SPH) method, this study provides a reliable and efficient tool for accurately analyzing fluid patterns and deriving hydraulic power losses within an acceptable industrial time frame of two days. The findings not only contribute to the understanding of loss sources and their physical origins but also highlight the potential of the SPH method for lubrication simulations and power loss optimization. Ultimately, the insights gained from this research will pave the way for reduced product development cycles and foster the use of efficient lubrication strategies in gearboxes.

Power losses within a gearbox are classified according to their component or origin, that is gears P_{LG}, bearings P_{LB}, seals, P_{LS}, and other parts or auxiliary components, P_{LX}, like clutches and electric pumps. Losses of the individual components are further divided into load-dependent, index L, and load-independent losses, sometimes referred to as spin or no-load losses, index 0. Following the notation of Niemann and Winter (Ref. 3), the power losses may be written as:

$$P_L = P_{LG} + P_{LG0} + P_{LB} + P_{LB0} + P_{LS} + P_{LX}. \tag{1}$$

Load-dependent losses are typically determined by standards or in-house or commercial gearing pre-design tools. On the contrary, accurate prediction of load-independent losses requires an accurate prediction of the interaction between lubricant and fluid which is a priori unknown as all components interact with the lubricant in a coupled manner. The load-independent losses are grouped by their physical origin. Churning, index C, arises due to the parts moving the inertia of the oil by pressure and viscous forces acting from the fluid towards the wheel. Squeezing, index S, covers losses that are generated by the rapid volume changes in the periodically opening and closing meshing zone. Windage, index W, covers losses due to air resistance. This yields the general formulation of load-independent losses in a passive lubricated gearbox:

$$P_{L0} = P_C + P_S + P_W. \tag{2}$$

It has been commonly observed that losses due to air resistance are negligible for circumferential speeds below approximately 20 m/s (Refs. 4, 5). This paper only covers losses due to the fluid's resistance to the gears and the bearing, ignoring the air's presence. This loss share covers the previously described churning and squeezing effects and will be addressed as hydraulic losses in this paper.

Although experimental research on the topic of gear power losses has been conducted since mid of the 20th century (Ref. 6) and extensive studies have been made in the following decades (Refs. 7, 8), no general concept has been developed to accurately determine power losses for all components in a transmission. The difficulty stems from the fact that the fluid flow within gearboxes is inherently complex. This is caused by the complexly shaped bodies churning through the lubricant-air mixture. The fluid phenomena for bevel gears are inherently more dynamic than cylindrical gears due to their exposed three-dimensional shape and mounting position. Only a little research on bevel gear churning losses has been conducted. Experimental studies on single rotating bevel gears made by Laruelle et al. (Ref. 4) propose a formulation for the churning torque over filling height, gear radius, and rotational speed for different fluid regimes. Quiban et al. (Ref. 9) updated these formulations and highlighted the phenomena of decreasing churning torques for dynamically varying filling heights. A broad range of tests for different hypoid gears, rotational speed, oils, attitudes, and single and meshing gears have been conducted by Jeon (Ref. 10). This study provides quantitative measurements for a specific gearbox. Therefore, his findings cannot be applied to arbitrary bevel-geared transmissions.

With the advent of high-performance computing and the progress of computational fluid dynamic (CFD) methods, simulations of the motion of the fluid within a gearbox became feasible (Refs. 11, 12). Subsequently, it was demonstrated that CFD is capable of accurately reproducing the fluid dynamics observed in experiments (Ref. 13). The investigations of the last decades are based on traditional CFD approaches that utilize a grid-based Eulerian technique. These methods are established but have to cope with major difficulties: With increasing complexity, that is more moving geometries, narrow gaps, and large geometry curvature, generating a sophisticated computational grid becomes difficult (Refs. 14, 15). Tracking the complex phase interface between air and oil requires a sufficiently fine mesh and the transient deformation of the domain with its moving parts requires adapting the grid over time. These demands raise the computational effort drastically. A variety of mesh and geometry handling techniques are employed to cope with this matter. A summary is given in Concli and Gorla (Ref. 16) and Concli et al. (Ref. 15). However, these methods have been proven to reliably predict churning losses in gears (Refs. 12, 13, 15). A sophisticated overview of state-of-the-art CFD research in numerical drivetrain lubrication applications is given in Maccioni and Concli (Ref. 17). It is carved out that individual methods exist to address hydraulic losses in bearings, gearsets, or pumps individually with more than 80 percent agreement between simulation and experiment. However, most of those papers focus solely on one of those mechanical components per simulation. Considering grid-based methods, e.g., Peng et al. (Ref. 18) presented qualitative results of an automotive rear axle gearbox with rotating bearings and validated their method with experimental values in a specialized test rig considering gears only. Oil, operating conditions, and filling heights are comparable to this paper. The simulation domain was separated into individual mesh zones, where motions were applied by user-defined functions. No detailed assessment of the bearing-induced churning losses is presented.

Smoothed Particle Hydrodynamics (SPH) is a Lagrangian CFD technique that has lower demands on geometry quality, thus decreasing simulation preparation time drastically. Mathematically, this approach renders a moving and deforming grid method where the collocation points are commonly called particles. Since neighboring relationships are updated after advecting the particles no computational grid is required. Here, particles of distinct fluid types represent individual phases and the unique particle type implicitly reconstructs the phase interface. Apart from the native handling of free surface flows, SPH has also proven to provide computational advantages for drivetrain simulations. Keller et al. (Ref. 19), as well as Maier et al. (Ref. 20), conducted SPH simulations 20–25 times faster than a Eulerian simulation of the same problem. These aspects indicate the significant potential of the SPH method in the field of transmission CFD. Being meshfree, it simplifies the time-consuming geometry preparation and the simulation itself, by making typical procedures such as remeshing or gear-scaling obsolete. Although overall fluid flow was reproduced accurately (Refs. 21–24) this method has not yet been proven to replicate the measured churning losses for various cases with an accuracy of over 80 percent (Refs. 17, 22). The main reason lies in under-resolving pressure gradients in the contacting areas and velocity gradients in churning regions. Multiple approaches with artificially increased fluid-wall friction are employed to calibrate results closer to the experimentally expected values. Contrary to the previous papers, the utilized SPH solver comes with the following differences:

- It imposes the boundary-particle interaction by considering the shape of the boundary, i.e., evaluating the boundary integral of the particle's kernel with the solid wall to ensure consistency of the kernel integration scheme. This is not ensured by employing dummy boundary particles or polygonal wall-distance-force functions (Refs. 25, 26) are used to describe the interaction of the fluid with the wall, which will inevitably lead to substantial spatial resolution dependencies.
- Using multiple particle resolutions per simulation to improve resolving the pressure gradients and fluid boundary layers.
- No usage of artificially increased forces between fluid-wall and fluid-fluid interaction to calibrate results to experimental data.

Moving particle semi-implicit (MPS) characterizes another Lagrangian CFD method. Both MPS and SPH are very similar in their numerical approach as shown in Soute-Iglesias et al. (Ref. 27). Again, multiple studies report accurate prediction of visual oil distribution within gearboxes (Ref. 25, 28). The churning loss determined by applying the MPS method on a high-speed railway system is qualitatively investigated in a similar study conducted by Deng et al. (Ref. 29) as well as in Shao et al. (Ref. 26). A similar qualitative study is presented in Singh et al. (Ref. 24). The results presented are derived from an implicit MPS solver that allows for theoretically larger time steps than the explicit SPH solver in this paper. However, implicit solvers have the disadvantage of solving the pressure Poisson equation by a computationally costly matrix inversion. Additionally, presented hydraulic losses for bearings were reported to be negligible low, i.e. one to two orders of magnitude smaller than the gear-induced hydraulic losses.

This paper outlines a methodology for investigating churning losses of gears and bearings simultaneously in an industrial gearbox by bridging the fluid scale differences with particle-refinement techniques in SPH and subsystem investigations of the bearings. A special focus is set on the importance of replicating the roller bearing's motion correctly instead of a simple rigid rotation. The method is applied as a parameter study considering rotational speed, turning direction, and filling height to highlight the benefits of cloud-native high-performance computing for virtually replicating experimental test rigs to derive a reliable system response within a few days without building a prototype.

Numerical Approach

SPH Kernel Interpolation

Fundamental to the SPH method is the spatially discrete representation of a continuum with so-called particles. These collocation points, which move along their trajectories, inherit the physical properties of the continuum.

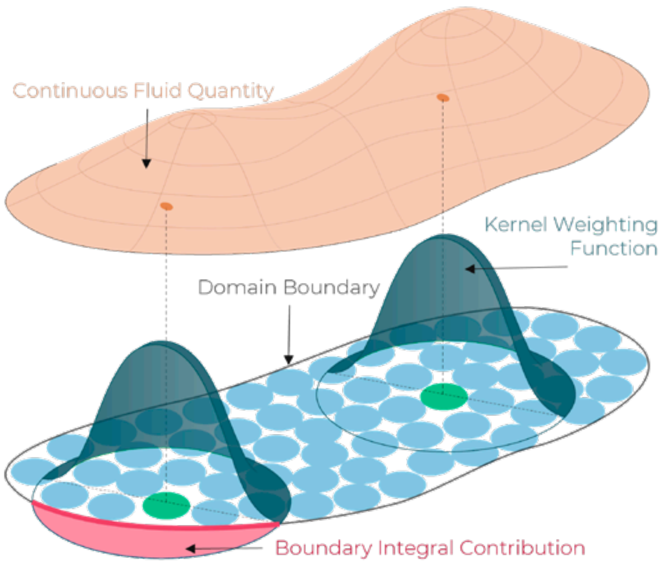

Figure 1—3D visualization of the SPH interpolation within the fluid (right) and with domain boundary contribution (left).

A weighted interpolation, i.e., the kernel function w, at these points, is used to determine its properties based on its distance from adjacent particles and their physical quantities ϕ. As the interpolation radius may extend beyond the presence of fluid, e.g., at walls, a renormalization factor γ is introduced to account for the missing content and ensure at least zeroth order consistency (Ref. 30). The described interpolation reads:

$$\phi(x_p) = \frac{1}{\gamma(x_p)} \int w(x_p - x)\phi(x)dV$$

$$\gamma(x_p) = \int w(x_p - x)dV \tag{3}$$

Here, the Wendland kernel of the fifth order is used as a weighting function. Using the derivative of the kernel, the SPH formalism allows for an approximation of spatial derivatives, which is crucial for solving partial differential equations numerically. The concept is illustrated in Figure 1. Specific care has to be taken for the consideration of boundary handling. Consider the lower green particle at position x_p then, with its kernel function w, the kernel interpolation of a derivative for arbitrary quantity ϕ will have a volume integral contribution ($\int \ldots dV$)and a boundary integral contribution ($\int \ldots dB$). The first comes from within the fluid, i.e., the contribution from the surrounding particles and the latter stems from the kernel overlapping with the wall. Here n is the inward-pointing surface normal. To ease readability, the renormalization term is ignored. Integration by parts yields (Ref. 31):

$$\nabla\phi(x_p) = \int \nabla w(x_p - x)\phi(x)dV - \oint w(x_p - x)\phi(x)n(x)dB \tag{4}$$

Navier Stokes Equations in a Weakly Compressible Formulatio

Liquids are considered incompressible if the density remains constant. This is true for fluid speeds significantly below the material's speed of sound or if pressures are not extreme. In the current work, a weakly compressible modeling approach is utilized allowing for small density changes, i.e., less than one percent. An equation of state links the pressure directly to the density change.

The mathematical basis of fluid dynamics is derived using this preposition. Incompressibility is considered for the derivation of the momentum equation. Contrarily, the continuity equation is solved in its compressible form to account for the change in the density. Here, the equation of state proposed by Cole (Ref. 32, 33) is used. This yields the governing equations for weakly compressible SPH in the Lagrangian formulation:

$$\frac{dx}{dt} = v$$

$$\frac{d\rho}{dt} = -\rho\nabla \cdot v$$

$$\frac{dv}{dt} = -\frac{1}{\rho}\nabla p + \frac{1}{\rho}\nabla \cdot \left(\mu\left(\nabla \otimes v + (\nabla \otimes v)^T\right)\right) + g$$

$$p = \frac{\rho_0 c_0^2}{\gamma}\left(\frac{\rho}{\rho_0} - 1\right)^{\gamma} + p_0 \tag{5}$$

with the position of the particles x, velocity v, time t, density ρ, pressure p, dynamic viscosity μ, gravity g, background pressure p_0, artificial speed of sound c_0, reference density ρ_0 and exponent γ, which is chosen as 7.0 for liquids like oil (Ref. 33) and 1.4 for gases like air (Refs. 34, 35). It should be noted that the artificial speed of sound is a numerical trick to enlarge the time step, i.e., fast computation times, while receiving physically sound results.

Equation 5 is discretized using the SPH formalism. The temporal derivates are discretized using a modified Runge-Kutta 4 (Ref. 37) scheme, separating the acoustic and advective time steps to allow for faster computation (Ref. 38). To improve numerical stability and the quality of the pressure field, an additional diffusive term is added to the continuity equation (Ref. 39). To ensure a regular particle distribution while avoiding unintended particle clumping, a particle shifting technique is applied (Ref. 40). This improves the interpolation quality of the scheme (Ref. 41) while maintaining the overall volume of simulated fluid. The utilized method is inspired by Ref. 42 and 43. In this work, no turbulence model is utilized.

Wall Boundary Conditions

For the wall boundary conditions, there are two major approaches to representation:

- The boundaries are thickened with so-called dummy particles, that can be included in the regular particle interaction (Ref. 32).
- Integral boundary conditions use a segment-based mesh representation of shapes (Ref. 44).

In Sabrowski et al. (Ref. 35], the different boundary condition approaches are discussed specifically for gearbox applications. This work uses a segment-based mesh representation to treat boundary conditions. This approach was chosen as it allows for a very accurate and native representation of computer-aided design (CAD) geometries in the SPH method and ensures to account for the boundary contribution of the SPH interpolation.

Particle Refinement Techniques

One of the five grand challenges of SPH is adaptivity (Ref. 45), which is generally the usage of multiple particle sizes within one simulation. The ideal particle-based solver adapts the particle size so that the numerical resolution is fine enough in areas of interest to resolve desired flow phenomena while being computationally fast and without introducing numerical errors. Having particles of different sizes interact in a naïve manner with one-another does immediately violate the conditions, such as:

- Larger particles would have larger kernel sizes, thus, considering smaller particles for the interpolation that do not see the larger particles. This would violate Newton's third law, i.e., reaction would not equal action,
- Compensating for this caveat by enlarging the kernel radii for smaller particles would lead to a significantly increase in particle neighbor count, thus, computational performance would decrease.

Multiple ideas exist like an adaptive particle splitting technique into multiples of their previous size based on certain pre-defined flow conditions. Similarly, these particles are merged, or de-refined. If the algorithm avoids the issues mentioned above, one idea can be to merge particles of versatile sizes as pairs or small groups. As pointed out by Chiron et al. (Ref. 46), this process can become computationally costly and faces difficulties when the coalescence rate differs from the refinement rate since particles may be merged as pairs but created as eightfold, twenty-sevenfold etc. An additional challenge is introduced as the de-refining step has been shown to react sensitively to non-regular fields (Ref. 45).

Another idea consists of small layers that coexist on top of the coarse domain to avoid overlapping of the kernels (Ref. 35). Here, the large, further denoted as coarse, particles enter the region of interest and, in the buffer layer of the fine particles, are split into finer particles. Fluid properties are interpolated into this layer by SPH formalism from active to passive particles ensuring information coupling of fine and coarse regions. Afterwards, the flow equations are solved on the fine particles and coarse particles are passively advected. Once the fine particles leave the buffer zone, the flow equations are solved by the reactivated coarse particles and the fine ones are deleted. This ensures mass conservation for the coarse layer. The process is schematically shown in Figure 2 and will be used in this paper.

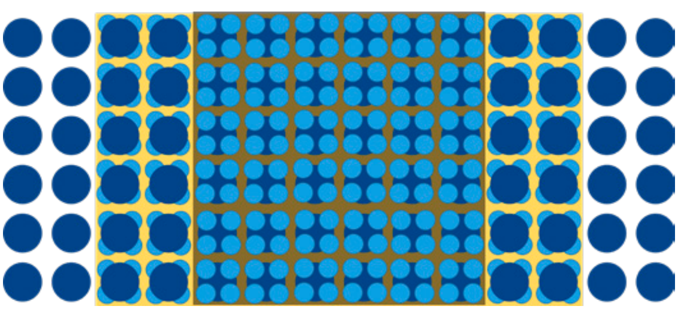

Figure 2—Particle refinement method with the multi-layer approach in 2D. Coarse particles are split into four fine particles in a buffer zone. The fine particles are active in the refinement zone.

Hydraulic Loss Evaluation Method

The calculation of churning losses is executed using pressure F_{pi} and viscous forces F_{vi} acting on the i-th rotating boundary triangle with area A_i and normal vector n_i as:

$$F_{pi} = p_i A_i n_i$$
$$F_{vi} = \mu \left(\frac{\partial v}{\partial x} \right)_i A_i n_i \tag{6}$$

The specific torque around the rotational axis of each component j can be calculated as:

$$T_j = \sum_i r_i \times (F_{pi} + F_{vi}) \tag{7}$$

with the lever r_i. However, a more general approach is exploited to calculate the local power P_i by its definition as force F acting on a segment scalar product with the segment velocity v_i:

$$P_i = v_i \bullet (F_{pi} + F_{vi}) = P_{pi} + P_{vi} \tag{8}$$

Integrating over the whole component leads to the corresponding overall power losses by means of viscous P_{vi} and pressure P_{pi}:

$$P_j = \sum_i (P_{pi} + P_{vi}) \tag{9}$$

which will be used to evaluate the power loss distribution for each component. Equation 8 circumvents the necessity to individually account for the torque of one roller bearing rotating around its axis and the axis of the shaft. This formulation is universally applicable.

Tapered Roller Bearing Kinematics

The kinematics calculation of the gears is done by applying an ideal gearing ratio and requires no further explanation. The bearing's motion is assumed to be slip and deformation free, thus, modelled by ideal kinematic slip conditions at the contacting surfaces. The equations must be derived in the form of two motions:

- The rigid rotation of the cage and rollers around the axis of the inner ring—ω_{cage}
- The rotation of each roller around its axis which is moved by the cage's motion—ω_{roller}

Since the motion of an axial, ball and cylindrical bearing represents a special case for a bearing with a roller that moves with tilted roller axes, a general set of motions is derived based on Figure 3.

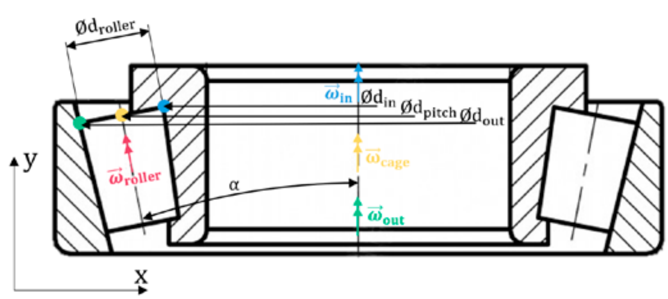

Figure 3—Schematic tapered roller bearing kinematic description.

The bearing moves slip free around the inner and outer race, thus, any set of points for a representative roller diameter suffices to derive the kinematic relationship. Without loss of generality, consider the three marked points (●, ●, ●). At the outer race (●), the circumferential velocity of the outer race must equal the superposition of the roller velocity added to the cage velocity. At the inner race (●), the circumferential velocity of the inner race must equal the superposition of the roller velocity subtracted from the cage velocity. Velocities are written in terms of rotational speed and effective diameter that yield:

$$\bullet\; v_{out} = \omega_{out}\frac{d_{out}}{2} = \omega_{cage}\frac{d_{out}}{2} + \omega_{roller}\frac{d_{roller}}{2} \tag{10}$$

$$\bullet\; v_{in} = \omega_{in}\frac{d_{in}}{2} = \omega_{cage}\frac{d_{in}}{2} - \omega_{roller}\frac{d_{roller}}{2} \tag{11}$$

Substituting $d_{in} = d_{pitch}$-$cos\ \alpha\ \ d_{roller}$ and $d_{out} = d_{pitch}$+$cos\ \alpha\ \ d_{roller}$ with α being the angle between the inner race axis and roller axis eventually leads to:

$$\omega_{cage} = \frac{1}{2}\left[\omega_{in}\left(1 - \frac{d_{roller}}{d_{pitch}}\cos\alpha\right) + \omega_{out}\left(1 + \frac{d_{roller}}{d_{pitch}}\cos\alpha\right)\right] \tag{12}$$

$$\omega_{roller} = \frac{1}{2}(\omega_{out} - \omega_{in})\left(\frac{d_{pitch}}{d_{roller}} - \frac{d_{roller}}{d_{pitch}}\cos^2\alpha\right) \tag{13}$$

Experimental Setup

The torque test bench *Kegelradprüfstand* (KRPS) at Dresden University of Technology (TUD) is used for this study. It consists of two slave and two test gearboxes of similar characteristics shown in Figure 4. Test gearbox 2 is investigated in detail. The load torque is applied on the pinion side, torque is measured with an HBM torque transducer of type T40B on the shaft of the pinion and as well as the wheel.

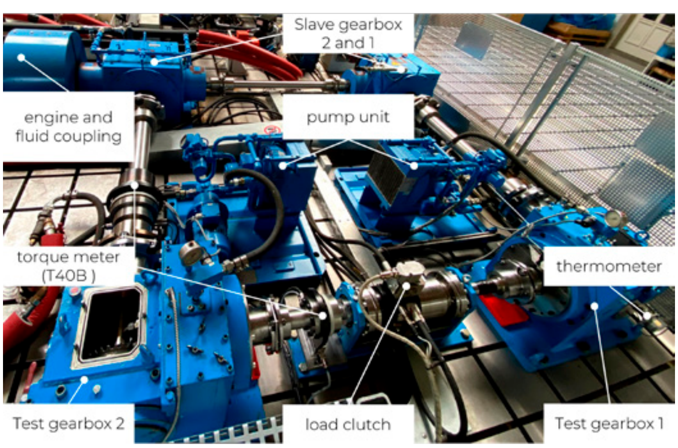

Figure 4—Bevel gear torque test bench (KRPS) at Dresden University of Technology.

The temperature was measured at the bottom of the oil reservoir. A temperature of 60 ± 2°C was ensured throughout all torque experiments. For the experiments, the oil Mobilube HD 80W-90 was used. The oil properties at the respective investigation temperatures are given in Table 1.

Temperature (°C)	Density (kg/m³)	Kin. Viscosity (cSt)
26	894	310
60	875	53

Table 1—Oil properties of Mobilube HD 80W-90 for the investigated operating conditions.

The test gearbox comprises a bevel gear stage with a gear ratio of 3.08. The pinion shaft is supported by two roller tapered bearings in the X-mounting position, the wheel is supported by two smaller tapered bearings in the O-mounting position and an additional cylindrical roller bearing. The digital model (Figure 5) does not include an active lubrication system in between the pinion bearings and the meshing zone as well as the pumping system and pipes at the bottom of the reservoir. This system cannot be removed nor switched off. Previous studies at the test rig have shown that the lubrication effect of the injection system is negligible. It is not clear if this holds for power losses as well. The uncertainty consequences are discussed at a later occasion.

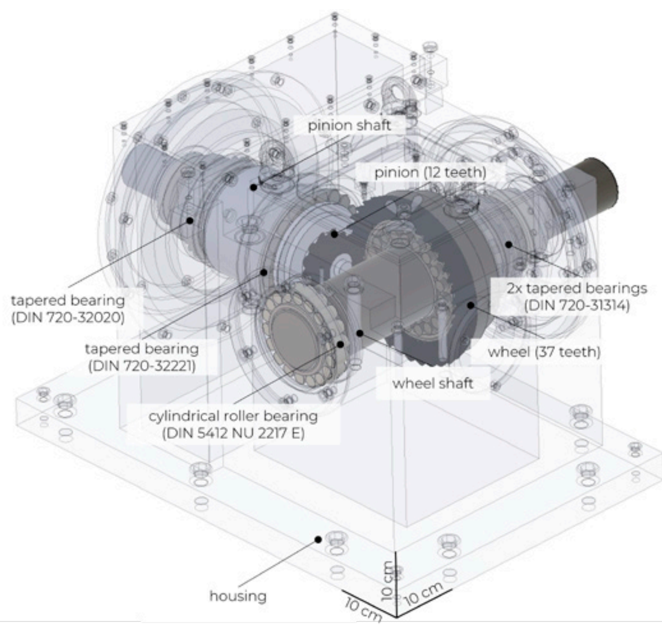

Figure 5—Geometry model of the test gearbox. Neither injection nor pumping system are included.

The average torque loss was measured for rotational speeds from 1,200 to 1,800 rpm, filling heights of 10, 45, and 85 mm below the centerlines and both turning directions. The gearbox of dimension 700 x 500 x 500 mm contains around 16 L oil at the highest filling level. The rotational speed was increased stepwise; this increase was followed by a stepwise decreasing measurement resulting in two torque readings that cover 15 seconds of measurement time each. The load-dependent, injection-induced and sealing losses were subtracted by employing one minimum lubricated test run for both turning direction. The introduced uncertainty is discussed at a later occasion. The gears are engaged in driving mode for all operating conditions. For all tests, a constant load of 1 kNm had to be applied on the pinion side to avoid damage to the slave gearboxes due to gear hammering. The following tests have been conducted for both turning directions, which is inwards (IN) if oil is immediately dragged into the meshing zone and outwards (OUT) otherwise. The gear characteristics are given in Table 2.

Parameter	Pinion	Wheel
Outside diameter d_0 (mm)	87.52	236.97
Mean pitch diameter d_p (mm)	66.96	206.46
Mean normal module m_{mn} (mm)	4.57	4.57
Number of teeth Z	12	37
Tooth width b (mm)	30	30
Tooth height h (mm)	10.28	10.28
Mean pitch angle δ (°)	17.97	72.03
Mean spiral angle β_m (°)	108.53	108.53
Generated normal pressure angle on drive side α_{nD} (°)	19.79	19.79
Spiral hand	Right	Left

Table 2—Bevel gear pair characteristics.

Numerical Setup

For a visual comparison, the cold start situation (26°C and 600 rpm) was captured by removing the top lid of the housing. The amount of aeration has been visually verified to be small after the test run. Visual validation of the oil distribution has been conducted by Ref. 36. For the following section, bearing DIN 720-32221 is addressed as the larger pinion bearing 1 (P1), bearing DIN 720-32020 is addressed as pinion bearing 2 (P2), bearing DIN 5412 NU 2217 E as wheel bearing 1 and both bearings DIN 720-31314 together as wheel bearing 2 and 3. Only the last two are provided with a cage geometry.

The simulations are executed as follows: Spatial particle refinement zones are located around the gears, bearings and the pinion's shaft between the supporting bearings as visualized in Figure 6.

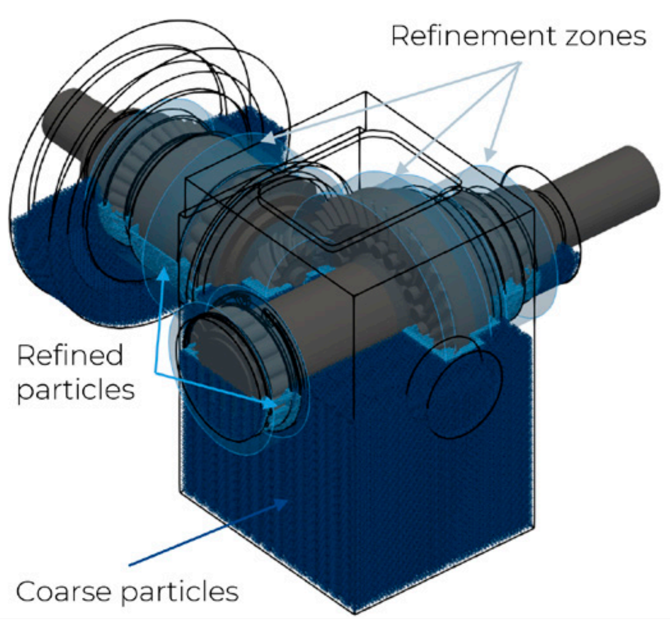

Figure 6—Initial discretization and geometry setup for nominal filling height of -10 mm below gear axes. Dark blue areas represent coarse particles (1.4 mm), light blue refined particles (0.7 mm). Transparent blue shapes indicate the refinement zones.

Both gears, shafts, and contacting roller bearings with cages linearly accelerate to full speed at 0.1 seconds and hold the terminal velocity for 0.4 seconds. The ramp-up is chosen to allow for faster quasi-stationary convergence. Starting with the terminal velocity introduces a shock similar to a splashing event into the simulation system whose effects take longer to decay. The movements of the bearings and cages follow the ideal kinematic contacting conditions. The simulation finishes at 0.5 seconds. The churning loss results are averaged over the last rotation of the wheel. The simulated hydraulic loss signal over time for a full system rotation of 1,600 rpm for the outward turning direction is shown in Figure 7. All simulations were conducted in parallel on the cloud-native simulation platform *Dive Solutions* on CPU AMD EPYC 7V73X within 29- and 40-hour simulation time with the solver *Dive SPH 3.4.1* with varying particle counts of 7 to 8.5 million.

The study Ref. 36 investigated the gear interaction space without bearings and found negligible loss differences for spatial resolutions smaller than 1.5 mm. To allow for a numerical discretization through the pinion and wheel shrouding gaps, a minimum global particle size of 1.4 mm must be chosen, which fulfils the particle size requirements of the study mentioned above. However, the previous study did not investigate the resolution sensitivity of hydraulic losses for the bearings or the shafts. Compared to the data presented in the study (Ref. 36) and this study the following differences are present:

- Postprocessing routine:
  - The newly utilized postprocessor reconstructs the exact forces present on the walls to accelerate the fluid.
  - The old, utilized postprocessor extrapolated the fluid-induced forces of interest from the fluid data onto the walls.
- Solver modelling:
  - A new particle-shifting technique has been used in this study.
- Spatial discretization:
  - Full system simulations were done with a 1 mm particle size in the previous study.

The consequences of these changes are manifold and cannot be summarized with a clear trend.

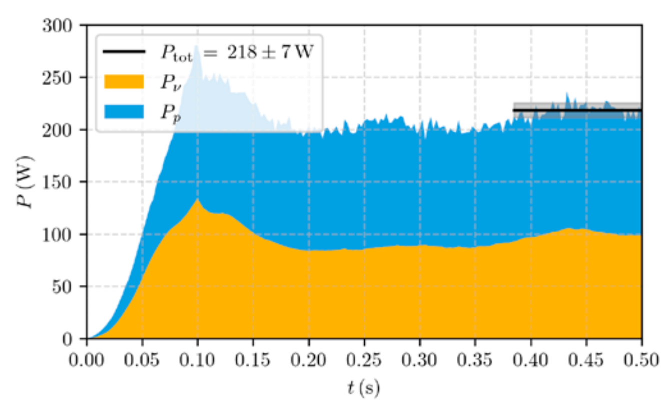

Figure 7—Viscous P_v (yellow) and pressure P_p (blue) induced hydraulic losses for the full system's OUT case without bearing subsystems at 1,600 rpm. Overall hydraulic losses are averaged over one full rotation of the wheel.

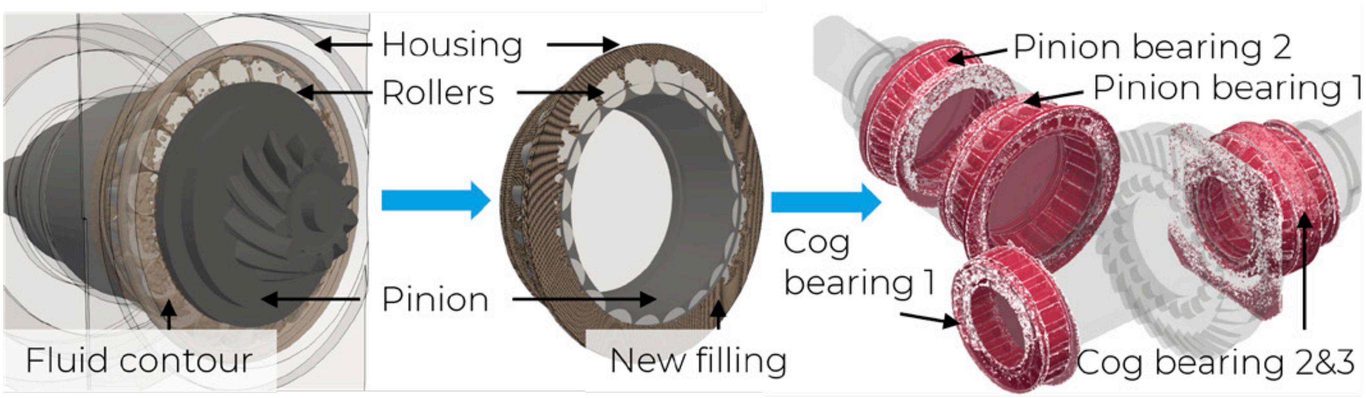

Figure 8—Visualization of the subsystem derivation step from a full system simulation (left) to a detailed system simulation of pinion bearing 1 (center) to all four subsystems (right).

The study Ref. 36 pointed out that the churning loss contribution from the tapered roller bearings in the pinion becomes substantial and needs to be captured. To keep the simulation effort low, the following method was employed: Based on the fluid distribution at the last output, the flow field around each bearing's proximity is extracted and further refined. This subsystem is investigated in a separate simulation until the results reach a stable value. The process is elucidated in Figure 8, where the fluid distribution's contour around the large roller bearing of the pinion is extracted and yields as a fluid filling for a subsystem simulation. To ensure mass conservation between the old and new system, the fluid contour is slightly thickened. The validity of this process is based on the assumption that a) the influence of the subsystem's axial boundaries is negligible and b) the loss signal becomes quasi-stationary before a significant amount of flow is moved axially through the bearing. Fixing the particle size globally at 0.25 mm for all bearing simulations lead to optimized runtimes of 0.5–4 hour per subsystem simulation for setups with 2 to 14 million particles allowing to complete all simulations within two days.

Starting the subsystems simulation from the derived fluid distribution at terminal speed induces a shock at the beginning of the simulation that quickly decays as shown in Figure 9 for the pinion's bearing 1 in the OUT case at 1,200 rpm. The pressure loss signal quickly starts to oscillate after the rollers covered one-sixth of the pinion shaft circumference at 12 milliseconds.

A side note on the observed oscillation frequency: it is fixed at around 120 Hz for this subsystem simulation. It does not seem to be related to the roller rotational speed around their axes (65 Hz) the roller frequency around the pinion (8.5 Hz), or the pinion's rotational speed (20 Hz). Similar effects were observed for the other bearing subsystems at 1,200 rpm and 1,600 rpm but not for 1,800 rpm at the given output frequency. The amplitude of this oscillation is relatively lower for the wheel's bearings compared to the pinion's bearings and is only visible at higher speeds. Lowering the oil level increases the amplitudes at a given rpm. The analysis of their origin is left for further research.

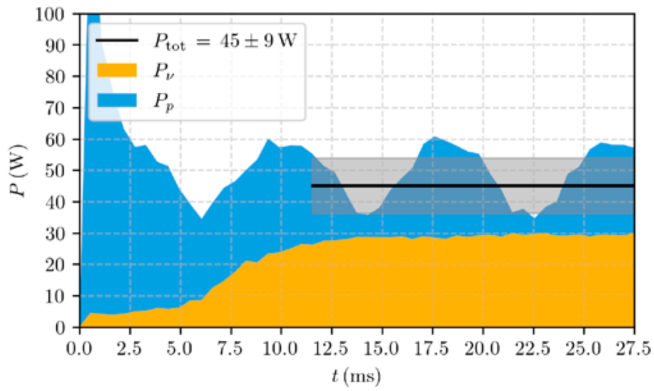

Figure 9—Viscous P_v (yellow) and pressure P_p (blue) induced hydraulic losses for rollers in the subsystem of pinion bearing 1 in the OUT case at 1,200 rpm. Overall hydraulic losses are averaged over 60 percent of the simulation length.

All consecutively shown data are combined results of the full system's pinion and wheel hydraulic losses and bearing subsystem analyses if not stated otherwise.

Results

Bearing Investigation

Modelling the ideal kinematics of bearings becomes challenging for grid-based methods to avoid degeneration of mesh cells and, thus, time convergence challenges. Even particle-based methods have lower geometry quality demands, so they are simulated with a simplified motion i.e., as a solid body rotating with the average of the relative rotational speed difference between the input and output shaft. The difference in terms of wetting and loss distribution of both approaches are investigated on the example of the pinions' bearings 1. To avoid the influence of surrounding geometries, both simulations were executed as a subsystem simulation from the fluid field of the 1,600 rpm-OUT case.

Time-averaged data is summarized in Table 3. Despite being less wetted, the ideal kinematics come with 67 percent higher hydraulic losses than the case with simplified kinematics. The reason for this difference is found in the negligible share of viscous losses for rollers under these kinematic conditions.

Component	Ideal kinematics	Simplified kinematics
Instantaneous wetting (%)	10 ± 0.2	14 ± 1
Pressure power losses (W)	41 ± 19	46 ± 2
Viscous power losses (W)	36 ± 2	0 ± 1
Total power losses (W)	77 ± 19	46 ± 3

Table 3—Instantaneous wetting and hydraulic power loss share comparison of pinion bearing 1 subsystem simulation at 1,600 rpm in the OUT case for ideal and simplified kinematics.

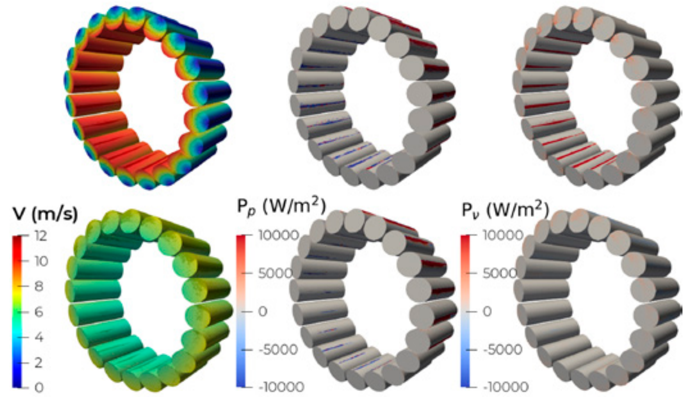

Figure 10—Comparison of the exact bearing kinematics (top) and a rigid rotation with half the shaft's velocity (bottom) in the subsystem simulation of pinion bearing 1 at 1,600 rpm, OUT, for velocity (left) with wetting- (shaded), pressure- (center) and viscous- (right) induced losses.

Considering the surface wetting distribution, pressure, and viscous hydraulic losses, in Figure 10, the shaded contours in the left column indicate a more wetted at the contacting zone at the outer race than on the inner race for both cases due to the general pumping behavior of a tapered roller bearing. The exact roller motion transports oil from the outer to the inner race and reduces the oil distribution shift. In contrast, the shift is more prominent for the simplified motion implying less oil on the inner race than on the outer race. Still, pressure-induced losses are of similar magnitude for the simplified motion despite having more oil at the outer race and a numerically higher velocity. For the ideal rolling motion a higher pressure is being built up by dragging the fluid on the surface into the contacting zone which counteracts the motion overall motion of all rollers. Since velocity equilibrium is enforced on the inner race, the same effect happens there but the pressure force acts beneficially in the direction of the overall roller's motion. In the simplified case, less fluid reaches the contacting area at the inner race. Combining this fact with lower speed leads to lower simulated pressured-induced losses.

While pressure-induced forces stem from a normal force counteracting the motion of the body, viscous-induced forces stem from forces acting tangentially against the direction of motion of the body. Keeping this in mind, fluid shear rates must be large in the contacting areas when the flow is dragged from the area of high volume into the area of low volume, thus, must escape elsewise. However, power losses are only produced in areas of high velocity due to the definition of power times velocity. At the outer race, the low velocity magnitude renders viscous induced power loss small but makes them substantially larger at the inner race for the correct bearing motion. For the simplified kinematics, the squeezing effect into the contacting zone is not captured, thus, viscous losses are negligible in case. At the inner race, the small amount of oil that reaches the contacting zone creates large friction on the shaft as this has a larger circumferential speed than the rollers.

An overview of viscous and pressured-induced loss changes from the full to the subsystem analysis is given in Figure 11 with the two largest bearing contributions, pinion bearing 1 (P1) and pinion bearing 2 (P2) and the loss change from the full system to the subsystem simulation. The change from 0.7 mm particle size resolution to 0.25 mm particle size becomes more prominent for larger rotational speeds indicating that larger speeds come with both higher velocity and pressure gradients. For an under-resolved simulation, i.e., velocity gradients are not captured at all, halving the particle size would lead to doubling the viscous loss share due to better resolution of the boundary layer. Here, the largest difference (1,800 rpm, OUT case, P1) is 2.5, which is lower than the particle size ratio of 2.8. Additionally, the wetting increased from 9 to 10 percent. Thus, boundary layers are partially resolved. The change in pressure can go both ways: for lower rpm, the pressure share on total losses reduces from coarse to fine resolution as particles are less as less geometrical squeezing appears. At higher rpm, resolving the physical squeezing in more detail reproduces the correct pressure gradients. Thus, ensuring convergence for both loss shares is paramount to determining convergence. More critically, under-resolving can lead to wrong trends as seen for the pinion bearing 2 trends from 1,600 to 1,800 rpm. The pressure share was not resolved at all. Thus 0.7 mm particle size is not sufficient to resolve pressure gradients in between the smaller rollers. Increasing the resolution did capture some pressure gradients and increased wetting by about five percent. A finer resolution is advised for future studies.

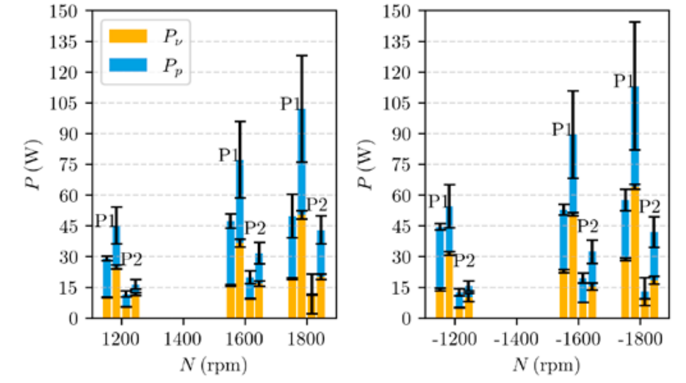

Figure 11—Viscous P_v (yellow) and pressure P_p (blue) induced churning losses by pinion bearing 1 (P1) and pinion bearing 2 (P2) in coarse (0.7 mm, left) and refined (0.25 mm, right) resolution over rpm. OUT (left chart) and IN (right chart) case are shown.

The subsystem simulation reveals that pinion bearing 2 is virtually unaffected by the turning direction. The measured amount of oil within the bearing is equal for all subsystems. Contrary, pinion bearing 1 churning losses are constantly more than 10 percent larger for the IN direction, more specifically, due to more than 15 percent larger viscous losses. This correlates with a more wetted area for the inward direction for all speeds for the direction of the inward as listed in Table 4. It is noticeable that a relative increase in wetting leads to a lower relative increase in viscous churning losses. Since the high viscous power loss zone—contacting zone of the roller at the inner race—is already filled, the additional wetted area is in regions of lower velocity gradients. A detailed investigation of the loss mechanism is given in the next investigation.

	Instantaneous wetting %	
Rotational speed pinion (rpm)	OUT	IN
1200	11 ± 0.3	15 ± 0.8
1600	10 ± 0.2	13 ± 0.8
1800	10 ± 0.2	13 ± 0.8

Table 4—Instantaneous wetting of pinion bearing 1 over rpm and turning direction.

Influence of Turning Direction

Turning direction is considered to have a substantial impact on hydraulic gearing losses. This effect is commonly known to be related to oil squeezing for high oil levels, specifically if an oversupply of oil is dragged into the gear meshing zone as could be expected for the IN case.

The simulations of both turning directions at 1,600 rpm input speed capture this trend as well—overall hydraulic losses are over 20 percent larger when oil is dragged into the meshing zone compared to out of the meshing zone. The same ratio was found in the experimental investigation. From Table 5, it is deducted that wheel bearing 2 and 3 as well as pinion bearing 2 are located away from the gear interaction zone, thus, losses are virtually unaffected by a change in turning direction. Although located in the gear interaction region, the cylindrical roller bearing on the wheel does not show a change in churning losses. Thus, the dynamic oil level change in the proximity of this bearing is not affected by the turning direction in this speed range. All components mentioned above are rotationally symmetric. Only asymmetrical flow towards the bearings due to asymmetrical geometrical changes close to these regions can cause noticeable differences in churning losses. Since pinion bearing 1, pinion and wheel interact with the fluid nearby, all differences are found for those three components. More specifically, all three components have larger losses in the IN case, with a 10 percent increase for the wheel, a 15 percent increase for the pinion bearing 1 and a 43 percent increase for the pinion.

Component	IN power losses (W)	OUT power losses (W)
Tapered bearings DIN 720-31314 (2x)	6 ± 0.2	6 ± 0.3
Cylindrical roller bearing D5412 NU 2217 E	6 ± 0.3	6 ± 0.3
Tapered bearing DIN 720-32020	32 ± 5	32 ± 5
Tapered bearing DIN 720-32221	89 ± 21	77 ± 19
Wheel	74 ± 12	67 ± 3
Pinion	115 ± 20	80 ± 5
Pressure power losses	149 ± 30	135 ± 20
Viscous power losses	173 ± 10	132 ± 4
Total power losses	322 ± 32	267 ± 20

Table 5—Component-wise load-independent power losses for the IN and OUT case at 1600 rpm pinion rotational speed.

The surface churning loss distributions for the gears are displayed in Figure 12. The wheel's loss contribution in the submerged section is more present for the OUT case than the IN case due to the beneficial teeth shape that guides oil with the wheel's motion. This oil is quickly thrown off the wheel towards the housing and a smaller share of the airborne oil falls or impinges at the housing close to the engagement zone. For the pinion, the same mechanisms apply with even less oil being guided back to the engagement zone due to the box-shaped housing.

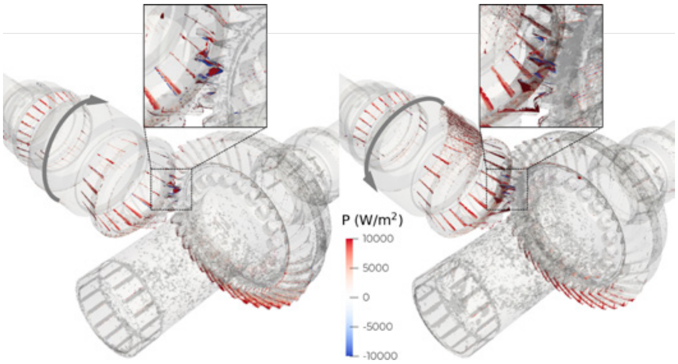

Figure 12—Churning loss distribution over the gears for 1,600 rpm at the input shaft in the OUT case (left) and IN case (right). Instantaneous wetting is indicated as shaded area. Zoom on the meshing zone on top.

On the contrary, the IN-case oil is piled up in the engagement zone due to the wheel pushing a substantial amount into this corner of the box (i, Figure 13). The difference in both clips represents over 75 percent more mass for the inward case in the region of interest. This excess oil is squeezed out of the engagement zone with the spin direction of the wheel into the pinion bearing 1. This explains why more oil reaches pinion bearing 1 in the IN direction than the OUT direction. Effectively, this effect also prevents oil from in between the pinion bearings to be pumped out leading to larger viscous losses around the large pinion shoulder (right, Figure 12). This effect comes also with larger viscous losses at the inner race, being part of the pinion (zoom, right, Figure 12). The oil is pumped out of the bearing at larger rotational angles (ii, Figure 13). Lastly, most of the oil is picked up again by the wheel and pushed to the opposite side of the housing (iii, Figure 13).

For the OUT case, oil that spun off the wheel, partially dripped back from the housing on the wheel and dragged into the engagement zone (1, Figure 13). There, it is axially squeezed towards the wheel shaft (3, Figure 13) leading to lower hydraulic losses due to the squeezing in this turning direction. As there is no large-scale flow created by the gears into the pinion bearing 1, less oil is pumped out of the bearing (2, Figure 13).

The main source—more than 50 percent of the increase—for additional losses in the direction of the inward stems from the pinion that a) has additional pressure contributions due to pushing more oil with the tooth flanks and b) larger viscous contributions due to more wetted area in between the pinion bearings and on the inner race of pinion 1.

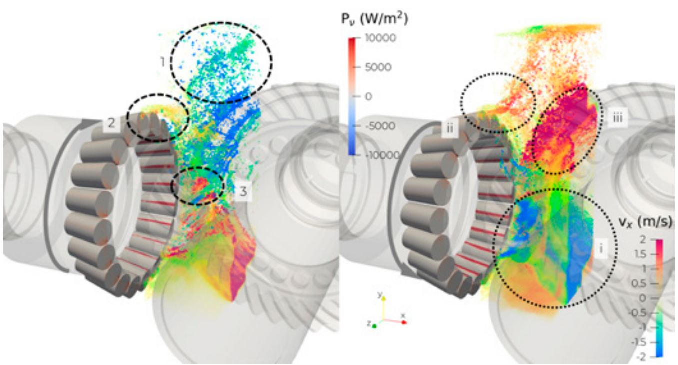

Figure 13—Clip of the axial velocity distribution in the gear engagement zone for 1,600 rpm at the input shaft in the OUT case (left) and IN case (right) with highlighted hydraulic loss mechanisms and viscous-loss distribution of pinion bearing 1.

The difference measurement for the experiment gave 510 W for the OUT and 610 W for the IN case as hydraulic losses of the system. Thus, the relative increase of 20 percent from outward to inward direction is replicated, however, the quantitative agreement is at 52 and 54 percent for the OUT and IN cases respectively.

Influence of Filling Height

Lowering the filling height is undoubtedly a simple measure to lower the hydraulic losses since gears are less submerged in oil. Table 6 summarizes the outcomes for an oil level immediately underneath the pinions' teeth. Simulated churning losses dropped by 27 percent, mainly due to a decrease in viscous loss contribution. Specifically, pinion churning losses plummet to 47 or 53 percent for the OUT and IN cases respectively. Considering the loss mechanism discovered in the previous section, those will be less present in cases where a) the pinion does not submerge in oil and b) fewer wheel teeth are immersed in the oil so less oil is dragged out from the reservoir. The splash pattern is still similar to the nominal filling height except for a lower oil column next to the engagement zone for the IN case at a lower oil level (Figure 15).

The simulation detects no change in hydraulic losses for the pinion bearing 2 in the subsystem simulation. Indeed, although the simulated masses for the pinion bearing 2 subsystems are 27 percent lower for the lowered level, the losses of the rollers show no change. The origin of this outcome is not clear as the rollers are indeed better wetted for the nominal filling height than for the lowered filling height, which is mainly found to be true for the front and back faces. As the main loss mechanism in the rollers was found to stem from the contacting region, the explanation might be that the pickup volume between the rollers is limited for a defined operating condition and not noticeably affected by filling height. Further research is required to understand this behavior.

Again, simulated losses are lower than the experimentally determined ones. With 270 W for the OUT and 370 W for the IN case difference measurements, experimental losses are met by 72 and 63 percent in the simulations of the OUT and IN case respectively.

	IN power losses (W)		OUT power losses (W)	
Component	-10 mm	**- 45 mm**	- 10 mm	**- 45 mm**
Tapered bearings DIN 720-31314 (2x)	6 ± 0.2	5 ± 0.2	6 ± 0.3	5 ± 0.2
Cylindrical roller bearing D5412 NU 2217 E	6 ± 0.3	5 ± 0.3	6 ± 0.3	5 ± 0.4
Tapered bearing DIN 720-32020	32 ± 5	33 ± 4	32 ± 5	32 ± 4
Tapered bearing DIN 720-32221	89 ± 21	78 ± 17	77 ± 19	70 ± 17
Wheel	74 ± 12	54 ± 4	67 ± 3	47 ± 1
Pinion	115 ± 20	61 ± 6	80 ± 5	37 ± 2
Pressure power losses	149 ± 30	122 ± 19	135 ± 20	123 ± 17
Viscous power losses	173 ± 10	112 ± 3	132 ± 4	73 ± 3
Total power losses	322 ± 32	234 ± 19	267 ± 20	195 ± 17

Table 6—Component-wise hydraulic power losses for the IN and OUT case at 1,600 rpm for the lowered oil level in comparison with the nominal filling height.

Influence of Rotational Speed

An overview of simulated losses over pinion rpm is given in Figure 14. Simulated losses increase with rotational speed. If 1,200 and 1,600 rpm results are considered, the simulated losses for 1,800 rpm exceed the linear extrapolation between both points indicating an over-proportional growth of churning losses with rpm with a maximum deviation of 7.5 percent. Still, for the simulated range, a linear trend is an acceptable simplification. If this trend is assumed, the linear least square regression yields a slope of (0.404 ± 0.006) W/rpm for the IN and (0.310 ± 0.032) W/rpm for the OUT direction. This observation is also valid for an artificial regression point of 0 W at 0 rpm. Therefore, simulated IN losses are not only larger than those in the OUT case but also grow 30 percent faster with rpm.

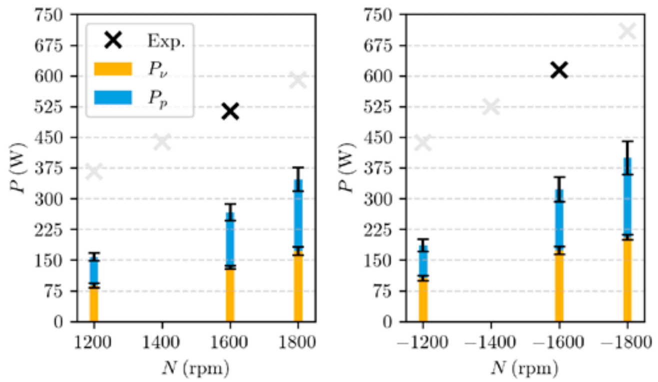

Figure 14—Viscous P_v (yellow) and pressure P_p (blue) simulated churning losses compared to experimental data (×) over rpm. OUT (left chart) and IN (right chart) case are shown. Bright marker indicate linearly extrapolated losses.

Part of this faster growth is likely to be seen in the wetting distribution and indicated surface flow direction Figure 15. While the wheel-induced splash pattern at the housing side opposing the pinion becomes more prominent for the OUT direction (-10 mm, left), this effect does not drive more oil towards the engagement zone of the gears (-10 mm, right). For the IN case, more is dragged upwards and against the housing in proximity to the gear meshing zone, which is a leading factor of churning losses (-10 mm, right).

The individual loss contributions show a different growth trend. Both contributions grow in absolute value with rpm, but pressure losses grow faster than viscous losses. As described in Ref. 36, pressure losses come with a higher order dependency on rotational speed, which is observed in this case as well.

The experimental trend is deducted from trends and not by measurements, thus, results with light grey crosses must be considered as estimates. For 1,600 rpm in both turning directions, load-dependent and load-independent losses were measured and losses with the same load but without any oil were deducted. The remaining difference accounts for hydraulic losses. As total losses followed a clear linear trend between 1,200 and 1,800 rpm for both directions, the measured delta has been scaled with rpm and deducted for all other operating conditions. This approach must yield a linear trend in hydraulic losses. Therefore, there is no additional value in comparing results for 1,200 and 1,800 rpm between simulation and measurement since results must be similar to the ones at 1,600 rpm.

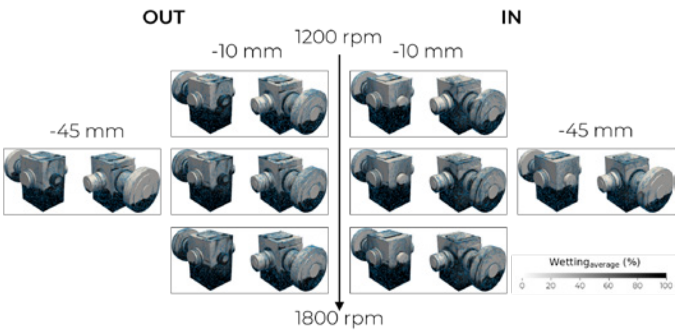

Figure 15—Average wetting on housing surface for OUT (left) and IN (right) case over pinion rotational speed and filling height. Flow paths are indicated with surface glyphs.

Experimental and Numerical Uncertainty Discussion

The difference in power losses from the filled and drained gearbox is considered to give hydraulic power losses. The results at the KRPS resulted in 610 W for the IN direction and 510 W for the outwards turning direction at 1,600 rpm pinion speed filling height 10 mm below the gear axes. The differences between the experiment to the simulation can be clustered as follows:

- Bearing representation:
  - Pinion bearings and the cylindrical roller bearing on the wheel come with cages which were not present in the CAD data.
- Measurement techniques:
  - Tapered roller bearings must be applied with preload, which results in loss contribution for both, load-dependent as well as load-independent classification.
  - The drained IN direction was investigated after the drained OUT direction was measured
  - Gear-load for 1 kNm to avoid gear hammering required a torque measurement device with high uncertainty for the differentially determined hydraulic loss range
- Active lubrication:
  - The test rig contains an active lubrication system injecting from above into the meshing zone and in between the pinion bearings. Neither is geometry present nor is the volume flow known.
  - This system cannot be shut down even with drained reservoirs.
- Oil properties:
  - Oil data was taken from the data sheet and not measured.
  - Oil reservoir temperature was considered as the overall oil temperature

For the simulation, the largest uncertainty is found to be the loss results in terms of particle size.

Starting with the bearings, including the cage is likely to increase viscous losses due to more area shearing the oil and squeezing in between the cage and rollers. It can be assumed that the cage can create an additional flow resistance leaving more oil in the zone between both pinion bearings. The effect is further increased by considering the active lubrication between the pinion bearings.

The assumption of oil properties could lead to changes in both directions. It can be assumed that this effect is of lower order both, oil properties of different charges and age as well as local temperature variation should not affect viscosity and density by significant factors.

Similarly, changes in pre-load with rotational speed or dynamic motion of the bearing may not account for a significant delta in the results. The large measurement device uncertainty may be ignored due to long measurement times and the assumption of result reproducibility. The order of drained measurement, on the other hand, can create substantial differences. After the drained test rig run for a few seconds at 1,600 rpm in the OUT case, the remaining lubrication film might have heated up or was even removed from the contacting surfaces. Higher temperatures would lead to lower viscosities, thus, lower friction coefficients. However, insufficient lubrication film thickness creates the opposite effect of mixed friction, thus, increasing losses. Since the measurement was done only once, this effect cannot be quantified and remains uncertain.

To summarize, the expected difference between the experiment and simulation setup would lead to lower simulated losses.

On the simulation side, it was carved out that resolving the boundary layer is paramount to replicating viscous-induced losses. As fluid shearing is a dominant loss source for this case, which mainly comes from bearings, inner races and the large churning shoulder of the pinion, these effects must be captured to achieve quantitative result parity with the experiments. The proposed simulation method with a) particle refinement in the global system and b) subsystem simulations in the bearings, helped to get closer to matching experimental values. What was not included in the results of this paper is the contribution of the pinion's shaft in the subsystem. Looking at the subsystem contribution from the inner race of pinion bearing 1 and 2, the inner races alone account in total for 63 and 89 W for the OUT and IN subsystem cases at 1,600 rpm case. These results did not consider the large churning shoulder. For the results presented in this paper, loss results for the pinion were extracted from the full system only, thus, noticeable higher values are expected for including the complete pinion's shaft including the inner races at higher resolution into the loss evaluation.

Conclusion and Outlook

In conclusion, the study focused on understanding the hydraulic loss mechanism and origins in a bevel-geared gearbox, to identify areas for constructive measures to optimize losses and enhance overall efficiency. The SPH method in a cloud-native environment proved to be a valuable tool for industrial use, offering fast turnaround times and reliable results in investigating fluid patterns, deriving hydraulic power loss trends and identifying options for optimization for a large set of operating conditions.

The findings revealed that churning power losses followed expected trends and ratios based on factors such as filling height, rotational speed, and turning direction. However, due to the dominant influence of viscous power losses in bearings and the churning shafts, the absolute values were underestimated as these phenomena are not yet fully resolved. However, the method of particle refinement in combination with bearing subsystem modelling proved to improve simulated results paving the way for further simulation advancements with more advanced spatial and temporal refinement techniques.

The results demonstrated the effectiveness of the SPH method in setting up lubrication simulations efficiently and generating accurate insights into loss sources and their physical origins. Given the complexity and interdependence of flow dynamics in bevel gear pairings with multiple bearings, empirical formulas proved to be case-dependent, further highlighting the robustness and advantages of the SPH method. Additionally, exploiting the robustness of the SPH method for setting up the exact kinematics of the bearings' motion makes it possible to avoid underestimating the effect of bearing churning losses with simplified motions. This study pointed out that not capturing the bearing motion properly can create severe result deviations.

The study emphasized that the SPH method offers significant benefits for reducing product development cycles, with its fast pre-processing, easy setup, accurate assessment of oil distribution and acceptable assessment of churning losses. Moreover, the method's ability to account for crucial parameters like rotational speed, turning direction, and filling instils confidence in secure A-B testing qualitatively and, with some limitations, quantitatively. Furthermore, the versatility of the SPH method extends beyond lubrication simulations, encompassing power loss optimization as well. Leveraging the cloud-based environment enhances the potential of SPH, allowing for simultaneous investigation of various operating points without limitations imposed by local hardware resources, effectively making it possible to conduct a study of 8 operating conditions with 32 subsystems in just two days. Experimental investigation would require similar time durations to measure, change and evaluate the results, not to mention the time to build and mount a functional prototype on the test bench.

Finally, the authors suggest applying a multi-layer and/or wall-bounded particle refinement around bearings and the pinion's shaft to get quantitative agreement and even higher accuracy in determining hydraulic losses of viscous origin. Future work should also cover the inclusion of heat sources and sinks such as load-induced losses from bearings and gears to determine the thermal limit of the gearbox.

PTE

Benjamin Legrady has been at Dive Solutions GmbH since 2020 helping engineers worldwide to achieve their business goals with Dive Solutions' cloud-native simulation platform and has served as a Customer Success Lead at Dive since 2022 leading sales engineering and post-sales. He holds a degree in Mechanical Engineering from Technische Universität Dresden.

References

1. Schlecht, B., 2010, *Machine Elements* (2nd engineer mechanical engineering). Pearson Studium, Hallbergmoos.
2. Polly, J. et al., 2008, "An Experimental Investigation of Churning Power Losses of a Gearbox," *ATZ Worldwide*, Vol. 110, No. 4, pp. 36–43.
3. Niemann, G. and Winter, H., 2003, *Machine Elements—Volume 2: General Gears, Gear Transmissions*, Springer, Berlin, Chapter: Basics, Spur Gears.
4. Laruelle, S. et al., 2017, "Experimental investigations and analysis on churning losses of splash lubricated spiral bevel gears," *Mechanics and Industry*, Vol. 18, No. 4.
5. Petry-Johnson, T. T. et al., 2008, "An experimental investigation of spur gear efficiency," *Journal of Mechanical Design: Transactions of the ASME*, Vol. 130, No. 6, pp. 0626011–06260110.
6. Ohlendorf, H., 1958, "Power loss and heating of spur gears," Dissertation, TH Munich.
7. Terekhov, A., 1975, "Hydraulic losses in gearboxes with oil immersion," *Bulletin of Mechanical Engineering*, Vol. 55, No. 5, pp. 13–17.
8. Mauz, W., 1987, "Hydraulic losses of spur gears at peripheral speeds of up to 60 m/s," Dissertation, Stuttgart.
9. Quiban et al., 2020, "Churning losses of spiral bevel gears at high rotational speed," *Proceedings of the Institution of Mechanical Engineers, Part J: Engineering Tribology*, Vol. 234, No. 2, pp. 36–43.
10. Jeon, S. I., 2010, "Improving Efficiency in Drive Lines: An Experimental Study on Churning Losses in Hypoid Axle,". Ph.D. thesis, Imperial College.
11. Arisawa, H. et al., 2009, "CFD simulation for reduction of oil churning losses and windage loss on aeroengine transmission gears," *Proceedings of the ASME Turbo Expo 1*, pp. 63–72.
12. Gorla, C. et al., 2013, "Hydraulic losses of a gearbox: CFD analysis and experiments," *Tribology International*, Vol. 66, pp. 337–344.
13. Mastrone, M. N. et al., 2020, "Oil distribution and churning losses of gearboxes: Experimental and numerical analysis," *Tribology International*, Vol. 151, p. 106496.
14. Liu, H. et al., 2017, "Determination of oil distribution and churning power loss of gearboxes by finite volume CFD method." *Tribology International*, Vol. 109, pp. 346–354.
15. Concli, F. et al, 2016, "A New Integrated Approach for the Prediction of the Load Independent Power Losses of Gears: Development of a Mesh-Handling Algorithm to Reduce the CFD Simulation Time," *Advances in Tribology 2016*, pp. 1–8.
16. Concli, F. and Gorla, C., 2016, "Windage, churning and pocketing power losses of gears: different modeling approaches for different goals," *Engineering Research*, Vol. 80, No. 3–4, pp. 85–99.
17. Maccioni, L. and Concli, F., 2020, "Computational fluid dynamics applied to lubricated mechanical components: Review of the approaches to simulate gears, bearings, and pumps," *Applied Sciences* (Switzerland), Vol. 10, No. 24), pp. 1–29.
18. Peng, Q. et al., 2018, "Investigation of the lubrication system in a vehicle axle: Numerical model and experimental validation," *Proceedings of the Institution of Mechanical Engineers, Part D: Journal of Automobile Engineering*, Vol. 233, No. 5, pp. 1232–1244.
19. Keller, M. et al., 2019, "Smoothed Particle Hydrodynamics Simulation of Oil-Jet Gear Interaction," *Journal of Tribology*, Vol. 141, pp. 1–7.
20. Maier, G. et al., 2019, "Requirements and limitations of traditional FVM and new SPH approaches for flow simulation in vehicle transmissions." *NAFEMS Magazine*, Vol. 52, pp. 42–52.
21. Groenenboom, P. H. L., Mettichi, M. Z., Gargouri, Y., 2015, "Simulating oil flow for gearbox lubrication using smoothed particle hydrodynamics," *Proceedings of International Conference on Gears*, Vol. 8, pp. 1–10.
22. Ji, Z., et al., 2018, "Numerical simulations of oil flow inside a gearbox by Smoothed Particle Hydrodynamics (SPH) method," *Tribology International*, Vol. 127, pp. 47–58.
23. Liu, H. et al., 2019, "Numerical modelling of oil distribution and churning gear power losses of gearboxes by smoothed particle hydrodynamics," *Proceedings of the Institution of Mechanical Engineers, Part J: Journal of Engineering Tribology*, Vol. 233, No. 1, pp. 74–86.
24. Menon, M., Szewc, K., Maurya, V., 2019, "Multi-Phase Gearbox Modelling Using GPU-Accelerated Smoothed Particle Hydrodynamics Method," *Proceedings of the ASME-JSME-KSME 2019 8th Joint Fluids Engineering Conference—Volume 3A: Fluid Applications and Systems*, pp. 1–10.
25. Singh, B., 2020, "CFD Simulation of Transmission for Lubrication Oil Flow Validation and Churning Loss Reduction," *SAE Technical Papers*, Vol. 2020-01, No. 1089, pp. 1–9.
26. Shao et al., 2022, "Investigations on lubrication characteristics of high-speed electric multiple unit gearbox by oil volume adjusting device," *J. Zhejiang Univ. Sci. A*, Vol. 23. pp. 1013–1026.
27. Soute-Iglesias, A. et al., 2013, "On the consistency of MPS," *Computer Physics Communication*, Vol. 184, No. 3, pp. 732–745.
28. Deng, X. et al., 2020, "Simulation and experimental study of influences of shape of roller on the lubrication performance of precision speed reducer," *Engineering Applications of Computational Fluid Mechanics*, Vol. 14, No. 1, pp. 1156–1172.
29. Deng, X. et al., 2020, "Lubrication mechanism in gearbox of high-speed railway trains," *Journal of Advanced Mechanical Design, Systems, and Manufacturing (Machine Design & Tribology)*, Vol. 14, No. 4.
30. Kulasegaram, S. et al., 2004, "A variational formulation-based contact algorithm for rigid boundaries in 2D SPH applications," *Computational Mechanics*, Vol. 33, No. 4, pp. 316–325.
31. Leroy, A., 2014, "A new incompressible SPH model: towards industrial applications," Ph.D. thesis, Université Paris-Est.
32. Adami, S., Hu, X. Y., Adams, N. A., 2012, "A generalized wall boundary condition for smoothed particle hydrodynamics," *Journal of Computational Physics*, Vol. 231, pp. 7057–7075.
33. Cole, H. R., 1948, *Underwater Explosions*, Princeton. New Jersey: Princeton University Press.
34. Grenier, N. et al., 2009, "A SPH multiphase formulation with a surface tension model applied to oil-water separation," Proceedings of the 4th SPHERIC International Workshop, Nantes, May 26–29, pp. 22–29.
35. Sabrowski, P., Beck, L., Wybranietz, T., 2019, "Modern WCSPH in industrial multiphase application considering complex moving boundaries," *Proceedings of the 14th SPHERIC International Workshop, Exeter, June 25–27*, pp. 266–273.
36. Legrady, B., et al., 2021, "Prediction of churning losses in an industrial gear box with spiral bevel gears using the smoothed particle hydrodynamic method," *Forschung im Ingenieurwesen*, Vol. 86, No. 3, pp. 379–388
37. Antuono, M. et al., 2012, "Numerical diffusive terms in weakly-compressible SPH schemes," *Computer Physics Communications*, Vol. 183, No. 12, pp. 2570–2580.
38. Zhang, C., Rezavand, M., and Hu, X., 2020, "Dual-criteria time stepping for weakly compressible smoothed particle hydrodynamics," *Journal of Computational Physics*, Vol. 404, pp.109–135.
39. Mayrhofer, C. et al., 2012, "Study of differential operators in the context of the semi-analytical wall boundary conditions," *Proceedings of the 7th International SPHERIC Workshop*, pp. 149–156.
40. Lind, S. J. et al., 2012, "Incompressible smoothed particle hydrodynamics for free-surface flows: A generalised diffusion-based algorithm for stability and validations for impulsive flows and propagating waves," *Journal of Computational Physics*, Vol. 231, pp. 1499–1523.
41. Oger, G., et al., 2016, "SPH accuracy improvement through the combination of a quasi-Lagrangian shifting transport velocity and consistent ALE formalisms," *Journal of Computational Physics*, Vol. 313, pp. 76–98.
42. Michel, J. et al., 2021, "Considerations on Particle Shifting Technique for SPH schemes," *Proceedings of the 15th International SPHERIC Workshop*, pp. 30–37.
43. Lyu, H. G. and Sun, P. N., 2022, "Further enhancement of the particle shifting technique. Toward better volume conservation and particle distribution in SPH simulations of violent free-surface flows," *Applied Mathematical Modelling*, Vol. 101, pp. 214–238.
44. Chiron, L., et al., 2019, "Fast and accurate SPH modelling of 3D complex wall boundaries in viscous and non viscous flows," *Computer Physics Communications*, Vol. 234, pp. 93–111.
45. Vacondio, R. et. al., 2021, "Grand challenges for Smoothed Particle Hydrodynamics numerical schemes," *Computational Particle Mechanics*, Vol. 8, No. 3, pp. 575–588.
46. Chiron, L. et al., 2018, "Analysis and improvements of Adaptive Particle Refinement (APR) through CPU time, accuracy and robustness considerations," *Journal of Computational Physics*, Vol. 354, pp. 552–575.

ABB
Supplies 1,300+ Robots for Volvo's Electric Vehicles

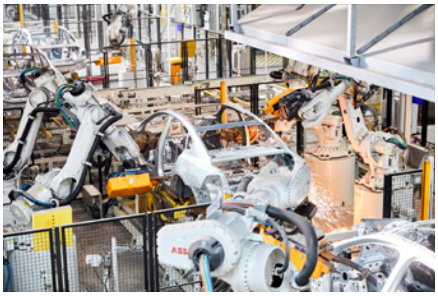

ABB is strengthening its long-standing partnership with Volvo Cars to supply more than 1,300 robots and functional packages to build the next generation of electric vehicles. This will support the Swedish car manufacturer to achieve its ambitious sustainability targets.

"The automotive industry's historic transformation, driven by increasing consumer demand for electric vehicles and a desire to operate more sustainably, is creating new opportunities as well as challenges for global manufacturers," said Marc Segura, ABB Robotics president. "This latest commitment from our partner Volvo Cars demonstrates our shared focus of delivering more sustainable manufacturing. Through our new, energy efficient large robot family and OmniCore controllers we will help to deliver energy savings of up to 20 percent at sites around the world."

This agreement includes functional packages covering various production tasks, from spot-welding, riveting, and dispensing to flow drilling and ultrasonic weld inspection. Each package is a ready-to-use, customer-proven combination of hardware, software and services and will be implemented at Volvo Cars' facilities in Torslanda, Sweden and Daqing, China. Alongside the hardware and functional packages, ABB's latest range of OmniCore robot controllers will help to deliver energy savings of up to 20 percent at sites due to their highly efficient power electronics and use of regenerative braking within the robot.

During the deployment, ABB will ensure production remains uninterrupted using its *RobotStudio* planning and programing software platform to visualize and optimize the deployment before the robots are installed. By developing and validating the required automation systems in a virtual space, Volvo Cars and ABB will create solutions that can be engineered once but deployed multiple times.

abb.com

FLENDER
Receives Supplier Award from Caterpillar

Drive specialist Flender has received the Supplier Excellence Recognition Award 2023 from U.S. machinery manufacturer Caterpillar. Flender received the award for maintaining 95 percent delivery reliability and zero defects. This achievement is awarded only to the top suppliers of Caterpillar. It positions Flender as a top supplier for its global Aftermarket (Reman) Division business.

Flender supplies new gearboxes, remanufactured gearboxes, spare parts, and couplings to Caterpillar for their 7495 Rope Shovel. Caterpillar created the certification program to recognize those suppliers who demonstrate their commitment to excellence and drive a zero-defect culture within their organizations. Suppliers are certified by meeting or exceeding stringent performance standards, including product quality and on-time delivery. Caterpillar's top-performing suppliers meet or exceed rigorous requirements and achieve world-class certification levels under Caterpillar's Supplier Excellence programming from May 2022 through June 2023.

"Caterpillar's reputation for world-class products and services stands on the shoulders of our global and diverse team—and that team includes our international and diverse supply network. By working together, we can deliver on our purpose to help our customers build a better, more sustainable world," said Pam Heminger, Caterpillar senior vice president for the strategic procurement and planning division. "We are very honored to receive the Supplier Excellence Award from Caterpillar for 2023 and to be recognized as one of their top suppliers. It reflects our long and outstanding partnership with Caterpillar. We look forward to continuing to deliver proven quality products for many years to come," said Kerry Klein, president, Flender Corporation.

flender.com

SPACE MACHINES COMPANY
Uses Siemens Software to Develop Orbital Servicing Vehicle

Siemens Digital Industries Software has announced that Space Machines Company (SMC), an Australian space on-orbit services and logistics startup, has used the Siemens Xcelerator portfolio of industry software to design and build the Optimus Orbital Servicing Vehicle. One of the largest commercial spacecrafts being designed, manufactured, and assembled in Australia, is in development at the University of Technology Sydney's Tech Lab.

The 270 kg Optimus will be launched by a SpaceX rocket from the United States to help taxi commercial satellites into their orbital paths around Earth and beyond—providing roadside assistance to satellites orbiting in space. Optimus' main purpose will be to service, maintain, repair and extend the life of other satellites in orbit.

SMC is using *NX* software for design and modeling, *Simcenter* software for thermo-mechanical elements simulation and analyses and *Teamcenter X* software as a service (SaaS) for cloud-based Product Lifecycle Management (PLM), which has helped reduce costs and time, while delivering productivity gains for teams working on Optimus.

"On-orbit servicing and logistics is the new frontier in space innovation. Many critical aspects of our daily lives, such as banking, weather forecasting and global communications are impacted by the ability of satellites to deliver these critical services. There are over 7,000 active satellites orbiting Earth. These satellites, and new ones coming into orbit, need a sustainable and safe operating environment. We deliver responsive and affordable on-orbit servicing and security solutions to customers," said Rajat Kulshrestha, CEO, Space Machines Company.

"To do what we do, we need the right software that is agile in a fast-paced environment and can scale as we do. Siemens' software has been critical in our ability to reduce design and development iterations without compromising on mission objectives. It's helped us create one unified digital environment and allowed us to rapidly prototype on the digital twin, helping us understand how Optimus will behave in orbit in unknown conditions."

Alongside the design and manufacturing phase, SMC's hardware and software undergo rigorous testing phases which calls for a robust PLM system. Teamcenter X helps with everything from quick design changes, running simulations and validation, through to manufacturing and final assembly—using Siemens' comprehensive digital twin.

"Space is one of the most innovative industries in Australia right now. Siemens software in enabling organizations of all sizes to innovate and develop solutions that will ultimately play a critical role in our daily lives," said Samantha Murray, vice president and managing director, Siemens Digital Industries Software, Australia and New Zealand. "I'm proud to see how Space Machines have used our software to push the boundaries of space logistics and get to the forefront of Australia's space industry. As the space industry scales up and becomes part of a powerful ecosystem, software is the key enabler that helps level the playing field for all."

sw.siemens.com

ATLANTA GEAR WORKS
Hires First HR Specialist

Atlanta Gear Works (AGW) is expanding its support staff by hiring its first Human Resources Specialist, a new position created to meet its expanding HR needs, previously managed by the company's chief financial officer.

"We're coming off one of our best years ever," said Atlanta Gear Works President Jack Conway. "As a company that's always invested in our people, we felt it was time to look at all of our employee benefits and policies, see what was still working and what needed changing. We knew we needed an experienced HR person dedicated to the role, and we were lucky to find Chelleigh."

Chelleigh [pronounced Shelley] Cuddy comes to Atlanta Gear Works with more than 15 years of HR experience in a variety of industries from the tech space to real estate, covering the entire employee experience from employee healthcare and other benefits to onboarding and offboarding new hires and terminations, establishing and streamlining internal processes for payroll and employee relations, and employee event planning.

"All of those positions made me stretch beyond my comfort level," she said, a trait she feels prepared her for the high-pressure world of gearbox repair, where an emergency repair can require an all-hands-on-deck 24/7 response.

Atlanta Gear Works designs, engineers, builds, rebuilds and repairs heavy industrial gearboxes for some of America's leading manufacturers with the goal of minimizing and preventing downtime. It also repairs other process-critical rotating equipment and continues to grow its field service division to provide extensive field machining and repair.

Among Cuddy's top priorities at Atlanta Gear Works are recruitment and an extensive employee policy and benefits review.

"Since starting at Atlanta Gear, I've been doing a lot of recruiting, revamping policies and looking at policy gaps that need to be closed and where we can improve benefits," said Cuddy.

In her first three months in her new position, she's attended at least one networking event a month, "getting our name out there, going to job fairs and career days."

One event that impressed her was a career day at a local junior high school, where she and AGW President Jack Conway set up a small trade show booth.

"We saw 300 kids, so many smart kids, kids that were interested and wanted to know about what we do," she said, calling it a "promising sign" given the widespread U.S. labor shortage.

atlantagear.com

ZF
Celebrates Production of Three Million Electric Motors

ZF has produced more than three million electric motors, a technology that is used worldwide in electric vehicles. ZF covers a broad spectrum of vehicle electrification: from purely electrically powered passenger cars and plug-in hybrids to electric drives for commercial vehicles. The production anniversary stands for a continuous reduction in the dependency on pure combustion engines as well as for the successful transformation to electromobility.

The global demand for electric drives for passenger cars and commercial vehicles is increasing rapidly—and so are ZF's production figures: "Within just 18 months, ZF has doubled electric motor production from just under one and a half million to three million," explains Roland Hintringer, head of the electric motors product line at ZF, adding: "Thanks to highly automated, volume-flexible and modular systems, we are able to serve our global customers as required."

Further innovations for more efficiency and range

The production figures and forecasts make it clear that ZF is successfully advancing the transformation towards electromobility. "Our role as an innovator is also an important factor," emphasizes Hintringer. ZF has already announced that it will develop the magnetic-free electric motor I^2SM—a separately excited synchronous machine with inductive energy transfer—for volume production which, in contrast to the magnetic-free concepts available on the market today, is uniquely compact and has the highest power and torque density. ZF has recently demonstrated the potential of ZF's new developments for further efficiency and thus range gains in electromobility with the EVSys800 electric drive: The prototype is 35 percent lighter than current electric drives and reduces CO^2 emissions in production and operation by 20 percent. Innovative stator winding technologies, a new cooling concept and the compact design make these major optimization leaps possible.

Worldwide production locations

ZF already produces electric motors at locations in Asia and Europe; production facilities are currently being installed in North America. The company thus serves the major automotive markets at the following locations: Hangzhou and Shenyang (China), Pancevo (Serbia), Schweinfurt (Germany), Trnava (Slovakia), Saltillo (Mexico), and Gray Court (USA). The capacities of the electric motor production facilities at the existing production locations are currently being expanded in order to best support the customers' ambitious sustainability and climate protection targets.

zf.com

CATERPILLAR
Announces Hydrogen-Hybrid Power Solution Program for Off-Highway Applications

Caterpillar has announced the launch of a three-year program to demonstrate an advanced hydrogen-hybrid power solution built on its new Cat C13D engine platform.

Starting in the first quarter of 2024, Caterpillar will develop a transient-capable system for off-highway applications. The project will demonstrate how state-of-the-art control systems and electric-hybrid components can help hydrogen-fueled engines meet or exceed the power density and transient performance of traditional diesel engines.

Caterpillar will serve as the prime contractor on the project, providing engine research and development as well as system integration. As the project progresses, other industry and academic collaborators will be brought into the program to provide additional specialist expertise. The initiative will be delivered at Caterpillar facilities in Chillicothe, IL, and San Antonio, TX.

With research commencing in 2024, the project is supported and partially funded by the US Department of Energy's (DOE) Vehicle Technologies Office (VTO) through the Office of Energy Efficiency and Renewable Energy (EERE). It is included among 45 projects across 18 states and Washington, DC, receiving funding to advance research, development, demonstration, and deployment in several areas critical to reducing greenhouse gas (GHG) emissions in the transportation sector.

The hydrogen-hybrid power demonstration project is the latest in a series of initiatives that builds upon Caterpillar's 35 years of enterprise experience in hydrogen fuels.

"Every off-highway application has its own unique duty cycles, lifecycle demands and performance expectations, and this complexity is driving the development of a wide range of power solutions for the energy transition," said Steve Ferguson, senior vice president Caterpillar Industrial Power Systems. "One size does not fit all, which is why we've engineered flexibility into the C13D engine to serve as our platform of the future."

cat.com

January 17–18

AGMA Involute Spline Design and Rating-Winter

This live online course will address both geometry and rating of involute splines of various types. The types of spline joints and their applications will be discussed. Spline configuration variations, including half depth, full depth, and special function designs, will be addressed. Both fixed and flexible spline configurations will be examined in terms of usage and design. Lubrication methods, including grease, oil bath, and flowing oil, as well as coatings appropriate for various spline applications, are examined. Shear and compressive stress rating methods are discussed with analyses methodology presented in both equation and graphical methodology via various rating charts.

powertransmission.com/events/968-agma-involute-spline-design-and-rating-winter

February 6–8

WestPack 2024

WestPack, Anaheim, CA, pairs design and packaging challenges with smart solutions in a setting that fosters interaction and inspiration. Pushing the boundaries of sustainability, environmental protection, and product vitality, WestPack brings together the leading packaging manufacturers from multiple industries, including food & beverage, medical device, pharmaceuticals, cosmetic and personal care, and electronics. Theater stages will cover topics such as sustainable packaging, medical device packaging, thermal shipping systems, sustainable cannabis packaging, food and beverage packaging and more. The event is co-located with MD&M, ATX West, D&M West, and Plastec West.

powertransmission.com/events/967-westpack-2024

February 13–15

Motor, Drive Systems & Magnetics 2024

MDSM (Orlando, FL) features the latest technical advancements in motor, drive systems, motion control, magnetic applications, technology, and rare earth materials. This is an opportunity for professionals to hear content in design, efficiency, and application advancements in automation, robotics, manufacturing, utilities, automotive, medical, consumer, aerospace & defense industries. Motor & Drive Systems is focused on the latest technical advancements impacting the design, integration, and efficiency of motor, drive systems, and motion control.

powertransmission.com/events/966-mdsm-2024

February 13–15

Industrial IoT Conference 2024

The Industrial IoT Conference (Ft. Lauderdale, FL) explores the potential of intelligent machines, prescriptive analytics, sensor driven analytics, and block chain solutions. Attendees learn about the industrial IoT technologies that are driving the transformation in manufacturing, supply chain and operations. Attendees include implementors, manufacturing companies, supply chain professionals, service providers, IoT manufacturers and more. Topics include implementation, warehouse logistics, robotics, sensors, cybersecurity, data analytics and more.

powertransmission.com/events/972-industrial-iot-conference-2024

February 22–24

IPTEX 2024

IPTEX 2024 (Pune, India) is an important event for all relevant stakeholders in automobile, aerospace, or energy as well as manufacturers, buyers, partners, and consultants. Focus industries include mechanical power transmission, electrical power transmission, linear motion drives, fluid power and IoT/smart technology. IPTEX will provide a consistent channel of communication to the members of this industry to come together under one roof and participate in technical seminars, share knowledge and expertise with industry leaders and to be a part of discussion on policy codes, standards and challenges faced by the industry.

powertransmission.com/events/964-iptex-2024

February 27–29

Gearbox CSI

This AGMA live online course examines individual failure modes and the failure scenarios that lead to actual system failure, an essential skill to designing gear/bearing systems that will operate properly for their full design life. In this course, AGMA will define and explain the nature of many gear and bearing failures and discuss and describe various actual failure scenarios. In addition, a detailed primer on bearing technology prefaces the failure scenario discussions. Attendees will gain a better understanding of various types of gears and bearings. Learn about the limitation and capabilities of rolling element bearings and the gears that they support. Grasp an understanding of how to properly apply the best gear-bearing combination to any gearbox from simple to complex.

powertransmission.com/events/969-agma-gearbox-csi

AD INDEX

BROWSE OUR BLOGS!

PTE features blogs to keep readers updated on the latest PT trends, technologies and industry solutions:

Bearings with Norm: After a several-years hiatus, we're pleased to welcome back our bearings blogger, Norm Parker.

Revolutions: Our editorial staff provides relevant and timely articles on a variety of PT industrial topics.

VISIT

powertransmission.com/blog/

CALL FOR PAPERS!

Are you sitting on an idea for a technical paper but wondering where to present it? Do you have one already written, sitting on your desk, gathering machine dust?

How about *Power Transmission Engineering*? We are always looking for gearing- and power transmission component-relevant technical papers for publication in the magazine and in its digital version. Having your work appear in *Power Transmission Engineering* guarantees you an audience of the most experienced and discriminating industry players. You say your work has not been peer-reviewed? Not a problem, as we are lucky — and thankful — to have on-hand some of the most experienced and brilliant minds in the industry — our technical editors. So if your work "passes muster" and is published, you'll know you were reviewed by the best — and most demanding.

Chances are you'll be creating the paper under the auspices of the company for whom you work or own, or for one of the various industry-relevant associations. That means they as well will bask in the reflected glory that accrues with publication in *Power Transmission Engineering*.

For publication guidelines and more information, please contact Randy Stott at *stott@agma.org*

Power Transmission Engineering® FREE SUBSCRIPTION

Respond TODAY *Your response ensures that we deliver the magazine only to those who want it. It also gives us the vital information we need to serve you best.*

24PTEALL

☐ **YES**
I want to receive/continue to receive ***Power Transmission Engineering***

☐ **NO**
Thanks anyway, but I don't need the world's best publication on mechanical components.

NAME: ______________________ **JOB TITLE:** ______________________

COMPANY: ______________________
ADDRESS: ______________________
(required)
____
CITY: ______________________
STATE/Province: ______________________
ZIP/Postal Code: ______________________
PHONE: ______________________

or Attach your business card here!

☐ ***Use home address below for delivery!***

ADDRESS: ______________________
____
CITY: ______________________
STATE/Province: ______________________
ZIP/Postal Code: ______________________

Signature: ______________________ **Date:** ______________
(required)

How would you like to receive *Power Transmission Engineering?*

☐ **PRINT** Version (Verify mailing info)
☐ **DIGITAL** Version (E-mail required) **You can OPT OUT at any time.*
E-MAIL: ______________________
☐ **BOTH** Print and Digital (Verify mailing info | e-mail required)

How is THIS LOCATION involved with power transmission products?

(Check all that apply)

☐ WE **MAKE** power transmission products
☐ WE **BUY** power transmission products
☐ WE **SELL** power transmission products (distributors, sales reps, etc.)
☐ WE **DESIGN** products with power transmission components in them
☐ Other (please describe) ______________________

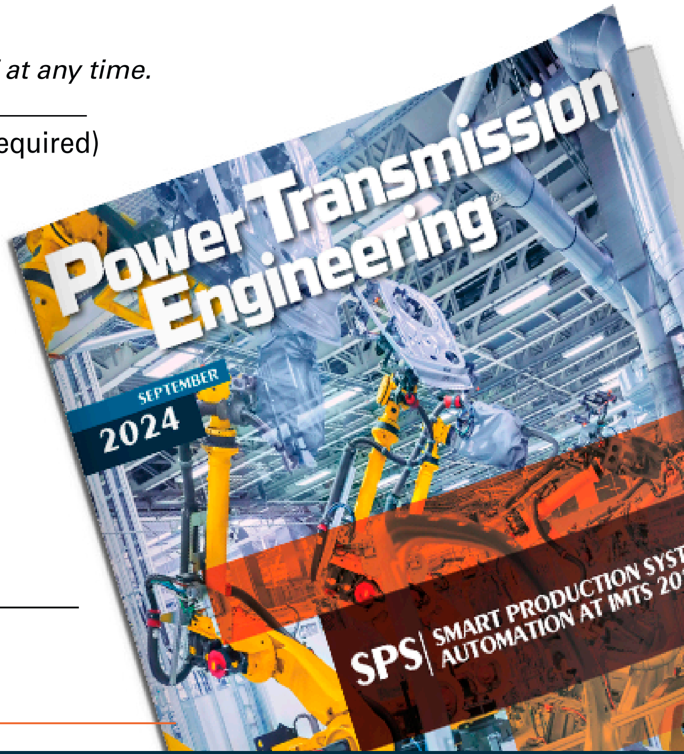

What is your company's principal product or service? ______________________

MAIL to: 1001 N. Fairfax St, Suite 500, Alexandria, VA 22314 USA | **SCAN to:** *subscribe@powertransmission.com* | **FAX to:** 1.847.437.6618

Flight of the Valkyries

Robonauts step from research to reality

Aaron Fagan, Senior Editor

NASA is in the process of designing humanoid robots for deployment to space including Valkyrie, which is amid final testing at the Johnson Space Center in Houston. While NASA states Valkyrie is being developed for "damaged or degraded environments" such as natural disaster sites, the agency designed the robot with the ultimate objective of serving off-planet missions. As these robots transition from research to reality, the societal and economic implications of integrating humanoid robots into the workforce are staggering.

The humanoid robot movement is in full swing, and the headline landscape is agog with companies such as 1X, Agility, Apptronik, Figure, Sanctuary, Tesla, and Unitree, all working towards commercially viable humanoid robots in 2024. Despite the latest reports of significant funding—for example, OpenAI-backed 1X reached $100 million Series B in January—a lack of recent fundamental technological breakthroughs, especially in actuators and batteries, poses challenges to the development of bipedal robots.

Valkyrie robot equipped with series elastic actuators (SEAs). Valkyrie specifically has five series-elastic rotary actuators and two linear actuators in the arms. Six finger and thumb actuators. Five series-elastic rotary actuators in the upper leg and two in the ankles. Five series elastic rotary actuators in the torso.

Series elastic actuators (SEAs), like those found in NASA's Valkyrie, are becoming commonplace in torque-controlled robots to achieve compliant interactions with environments and humans alike. The challenge is to make robots more efficient in how they move and respond to external forces, requiring a control system that optimizes their stability and performance. Striking a balance between two aspects of the control system allows the robot to perform various tasks effectively.

The software behind humanoid robots is becoming increasingly sophisticated. NASA's engineers have indicated a design such as Valkyrie would eventually have the same dexterity and functionality as human operators, completing tasks such as solar-panel maintenance or equipment repair.

Robonauts are taking on increasingly dexterous and intricate tasks aboard spacecraft to offer astronauts freedom for exploration and discovery. Shaun Azimi, NASA Dexterous Robotics Team Leader, has indicated the objective is to relieve astronauts of mundane, dangerous tasks, not to supplant them.

NASA is partnering with robotics companies like Austin-based Apptronik to learn how humanoid robots developed for terrestrial purposes could benefit future humanoid robots destined for space.

Apptronik is developing Apollo, a humanoid robot whose earthly tasks will include working in warehouses and manufacturing plants by moving packages, stacking pallets, and other supply chain-oriented tasks. The company plans to start providing humanoid robots to companies in early 2025.

"Robots like Apollo are designed with modularity in mind to be able to adapt to many applications," Azimi said. "And that's where NASA's trying to get that insight—to see what the key gaps are, where we would need to invest in the future to bring a terrestrial system into the space environment and certified for operating in space."

Valkyrie was sent to Australia this past summer for preliminary tests of its dexterity and handling capabilities on an offshore oil rig, where it was used as a "remote caretaker" for uncrewed, offshore energy facilities.

PTE

NEW MINIATURE BALL SCREWS

Solve Supply Chain Issues

with State of the Art CNC Roll Threaded Ball Screws

Miniature ball screw assemblies from PBC Linear have a range of leads with small screw diameters for high precision linear motion. Our ball screws are precision-rolled to achieve lead accuracy and consistency over the full length of the screw.

Manufactured at our Midwest headquarters allows for short lead times in compared to overseas sources.

- **Available Sizes** - Flange and Cylindrical Nuts

6 x 1 | 8 x 1 | 8 x 2 | 8 x 2.5 | 10 x 2

- **Internal Ball Screw Return System** — Multiliner System

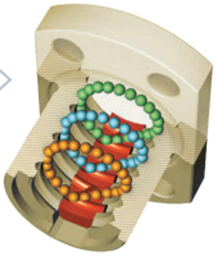

- **Machined Journals**

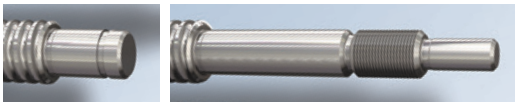

- **State of the Art Metrology and Inspection**

- **Integrated Ball Screw Motors**
  - NEMA 08, 11, 14, 17, & 23

- **Customization Available**

- **Applications**

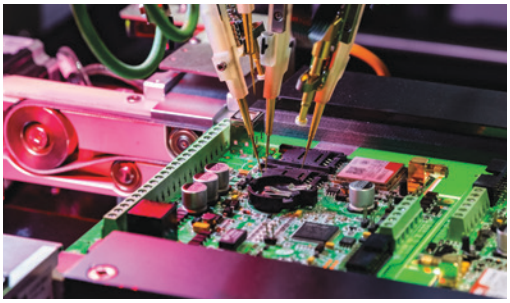

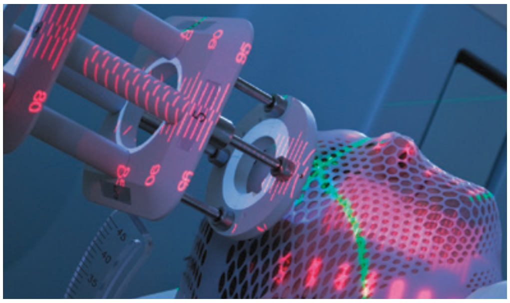

bit.ly/BallScrew2024

PBC Linear®

6402 E. Rockton Road, Roscoe • Illinois 61073 USA • +1.800.962.8979 • pbclinear.com